Journal of Medicinal Chemistry

pubs.acs.org/jmc

Article

Discovery of 2-(3-(3-Carbamoylpiperidin-1-yl)phenoxy)acetic Acid Derivatives as Novel Small-Molecule Inhibitors of the β-Catenin/B-Cell Lymphoma 9 Protein−Protein Interaction

Zhen Wang,[‖] Min Zhang,[‖] Wen Luo, Yongqiang Zhang, and Haitao Ji*

Cite This: J. Med. Chem. 2021, 64, 5886−5904

Read Online

ACCESS | Metrics & More | Article Recommendations | Supporting Information

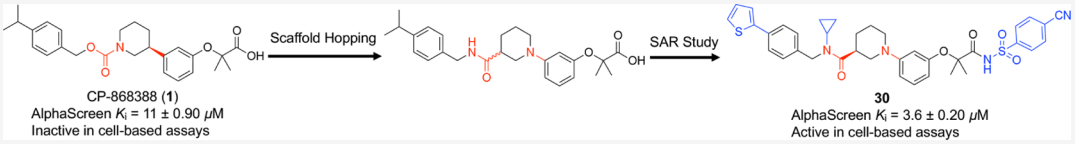

ABSTRACT: The β-catenin/B-cell lymphoma 9 (BCL9) protein−protein interaction (PPI) is a potential target for the suppression of hyperactive Wnt/β-catenin signaling that is vigorously involved in cancer initiation and development. Herein, we describe the medicinal chemistry optimization of a screening hit to yield novel small-molecule inhibitors of the β-catenin/BCL9 interaction. The best compound **30** can disrupt the β-catenin/BCL9 interaction with a K_i of 3.6 μM in AlphaScreen competitive inhibition assays. Cell-based experiments revealed that **30** selectively disrupted the β-catenin/BCL9 PPI, while leaving the β-catenin/E-cadherin PPI unaffected, dose-dependently suppressed Wnt signaling transactivation, downregulated oncogenic Wnt target gene expression, and on-target selectively inhibited the growth of cancer cells harboring aberrant Wnt signaling. This compound with a new chemotype can serve as a lead compound for further optimization of inhibitors for β-catenin/BCL9 PPI.

INTRODUCTION

The canonical Wnt pathway participates in various biological processes including embryogenesis, tissue homeostasis, and stem cell renewal.[1,2] In unstimulated cells, the protein β-catenin, a central hub of this pathway, undergoes constitutive degradation guided by the destruction complex consisting of Axin, casein kinase 1α (CK1α), adenomatous polyposis coli (APC), protein phosphatase 2A (PP2A), and glycogen synthase kinase 3β (GSK3β), and thus, free β-catenin is maintained at the undetectable-to-baseline levels. Upon activation of the Wnt signal by a Wnt ligand, the destruction complex disassembles and β-catenin is liberated. Free β-catenin accumulates in the cytosol in its dephosphorylated state and enters the cell nucleus, where β-catenin interacts with the lymphoid enhancer-binding factor (LEF)/T-cell factor (TCF) and binds with B-cell lymphoma 9 (BCL9)/BCL9-like (BCL9L), p300/CREB-binding protein (CBP), and Pygopus (Pygo 1 or Pygo 2) and among other co-activators to activate β-catenin target genes.

Aberrant activation of Wnt/β-catenin signaling has been recorded in many cancers.[3−6] For example, *APC* mutations and truncations that lead to β-catenin accumulation were detected in ∼80% of colorectal cancer.[7] *AXIN* with loss-of-function mutations was observed in esophageal squamous cell carcinoma, hepatocellular carcinoma, and colorectal cancer.[8−10] Oncogenic β-catenin activation mutations were described in colorectal cancer, hepatocellular carcinoma, prostate cancer, thyroid tumor, and ovarian endometrioid adenocarcinoma.[11−15] The autocrine/paracrine secretion of upstream effectors or the epigenetic silencing of the genes of negative regulators of the Wnt pathway also activates the Wnt/β-catenin signal and has been reported for various types of cancers.[16−22] In addition, aberrant β-catenin signaling plays a critical role in cancer immune evasion and immunotherapy resistance.[23−29] This collective evidence strongly supports the suppression of hyperactive Wnt/β-catenin signaling as a new direction for developing anticancer drugs.

The upstream effector proteins of the Wnt/β-catenin cascade have been extensively targeted by various therapeutic agents.[30−35] However, these agents are expected to be ineffective against cancer cells with more downstream genetic or epigenetic mutations, such as loss-of-function mutations of *APC* and *AXIN* or activation mutations of *CTNNB1* (β-catenin target gene). Furthermore, some of these agents might cause off-pathway effects given that their targets (GSK3β, tankyrase, and CK1α) are upstream and involved in multiple cellular processes. The β-catenin/BCL9 complex, located in the β-catenin-containing transcriptional supercomplex, appears to be a promising target to suppress hyperactive β-catenin signaling. The protein−protein interaction (PPI) between β-catenin and BCL9 is significantly upregulated in tumor tissues, and murine gut

Received: January 11, 2021
Published: April 27, 2021

BCL9/BCL9L elimination did not lead to overt phenotypic consequences or affect normal intestinal homeostasis, indicating that targeting this PPI might have no or very low toxicity.[36,37] BCL9/BCL9L knockdown by siRNAs and shRNAs significantly suppressed the growth of cancer cells that depend upon β-catenin signaling in vitro and in vivo.[36,38] BCL9/BCL9L conditional ablation induced differentiation and totally abolished tumorigenicity of murine intestinal organoids, while exhibiting no effect on cell proliferation.[39] More importantly, BCL9/BCL9L loss blocks tumorigenesis driven by Wnt signaling and extends disease-free survival in models that recapitulate human cancer.[40,41] These data suggest that targeting of β-catenin/BCL9 PPI holds great promise for treatment of cancer.[40]

Apart from peptide-based inhibitors,[42−45] two series of small-molecule disruptors have been reported for β-catenin/BCL9 PPI.[46−49] Carnosic acid (Figure 1) was reported as an inhibitor

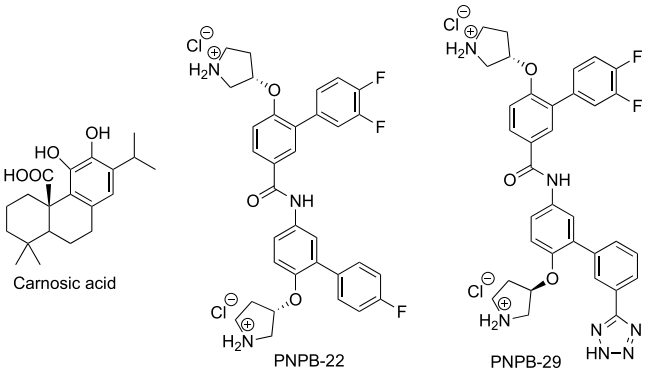

Figure 1. Reported small-molecule β-catenin/BCL9 disruptors.

of β-catenin/BCL9 PPI after screening two compound libraries by Bienz and coworkers.[46] Recently, our group reported 3-(4-fluorophenyl)-*N*-phenylbenzamide (PNPB) derivatives in Figure 1 as β-catenin/BCL9 inhibitors by rational design and optimization.[47,48] While the existing scaffolds contain some challenges for further inhibitor optimization, it is highly desirable to discover new small-molecule inhibitors with novel scaffolds to disrupt β-catenin/BCL9 PPI for chemical biology and anti-cancer drug discovery studies. Herein, we disclose a class of new selective small-molecule disruptors of the β-catenin/BCL9 interaction.

RESULTS

Inhibitor Design and Optimization. Our medicinal chemistry program started with a hit compound, CP-868388 (**1**), discovered by compound screen using the AlphaScreen competitive inhibition assay.[50] Compound **1** after resynthesis inhibited the PPI between full-length β-catenin and BCL9 with a K_i of 11 μM in AlphaScreen assays. The robustness of this AlphaScreen assay using full-length β-catenin is described in Figure S1. Given that the carbamate group in **1** is liable to metabolic hydrolysis[51] and the chiral carbon is difficult to construct,[52] the scaffold-hopping strategy was adopted to obtain a new scaffold, as shown in compound **2** (Table 1). Inhibitor **2** displayed a K_i of 71 μM for inhibiting the β-catenin/BCL9 interaction. Although **2** is about sixfold less potent than **1** for β-catenin/BCL9 inhibition, the amide group in **2** is more stable and the synthetic accessibility toward **2** is much higher, and thus, **2** is a reasonable starting point for further modification. Initial efforts were made focusing on the amide bond, and after synthesis, the inhibitory activity results of the derivatives are summarized in Table 1. Compound **4** with a methylated amide showed a slightly improved potency over **2**. Increasing the size of substituents on the amide [from methyl (**4**) to ethyl (**5**), isopropyl (**6**), and cyclopropyl (**7**)] resulted in further improvement on inhibitory activity, with compound **7** being the most potent derivative. The K_i value for **7** is 36 μM and twofold better than that of **2**. Compound **3** with one more methylene group between 4-isopropylbenzyl and amide was also synthesized, and it turned out to be slightly less potent than **2**.

To further improve inhibitory activity, various heterocycles were introduced in the position of the isopropyl substituent to explore more interactions with β-catenin. The results showed that compounds bearing nitrogen-containing heterocycles (**8**, **9**, **10**, and **11**) displayed potency loss when compared with **7** (Table 2). Compounds with the furan moiety (**14** and **15**) were also less potent than **7**, while compounds **12** and **13** bearing thiophene showed increased activities (Table 2). For example, compound **12** with 2-thiophene inhibited the β-catenin/BCL9 interaction with a K_i of 13 μM, which is threefold more potent than **7**. Notably, **12** is as potent as the hit compound **1** in the AlphaScreen assay.

Although compound **1** inhibited the β-catenin/BCL9 interaction with a K_i of 11 μM in AlphaScreen assays, it was inactive in cell-based experiments.[50] Careful examination on the chemical structure of **1** suggested that the inferior cellular activities might be caused by the carboxylic acid moiety, which is known to negatively impact cell membrane permeability. Consistently, the MTS assay revealed that **12** bearing the same carboxylic acid group showed very low inhibitory activities on viability of cancer cells (Table 5), although it displayed a K_i of 13 μM in AlphaScreen assays. Therefore, further optimization was conducted on this carboxylic acid group to improve both biochemical and cellular activities. Compounds **16** and **17** featured with methyl and *tert*-butyl esters, respectively, were synthesized (Table 3), and both compounds showed significant potency loss. This result indicated that the negative-charge character of the carboxylic acid group was important for maintaining the inhibitory activity. Based on this observation, a bioisosteric replacement strategy was adopted, and a series of *N*-acyl sulfonamide derivatives were designed (Table 3). *N*-Acyl sulfonamide is a well-known bioisostere for carboxylic acid and often employed to obtain derivatives with improved cell permeability, higher binding affinity, and better metabolic stability.[53] The first designed compound **18** with a *N*-acyl methanesulfonamide group inhibited the β-catenin/BCL9 interaction with a K_i of 21 μM and was twofold less active than **12**. Encouragingly, the substitution of the methyl group in the *N*-acyl methanesulfonamide moiety with larger substituents [such as cyclopropyl (**19**), isopropyl (**20**), and phenyl (**21**)] led to derivatives with improved activities. For example, compound **21** with *N*-acyl benzenesulfonamide displayed a K_i of 6.4 μM, and it is twofold more potent than **12**. To improve the physicochemical properties of these inhibitors, hydrophilic substituents including methoxy, hydroxy, and cyano moieties were introduced to the phenyl group of *N*-acyl benzenesulfonamide. As shown in Table 3 and Figure S2, these compounds showed increased activities when compared with **21**. Specifically, compounds **22** and **26** displaying K_is of 4.1 and 3.9 μM, respectively, were the two most potent inhibitors. Finally, the *R*- and *S*-isomers of **22** and **26** were synthesized, and their preliminary activities were determined in AlphaScreen assays.

https://doi.org/10.1021/acs.jmedchem.1c00046
J. Med. Chem. 2021, 64, 5886−5904

Table 1. AlphaScreen Assay Results of 1−7[a]

Compounds	Structure	IC_{50} ± SD (μM)	K_i ± SD (μM)
1 (CP-868388)	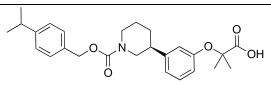	12 ± 1.0	11 ± 0.90[b]
2	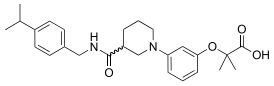	83 ± 15	71 ± 11
3	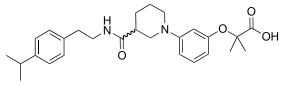	92 ± 23	82 ± 20
4	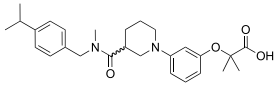	71 ± 6.2	59 ± 5.2
5	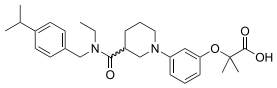	59 ± 2.8	50 ± 2.5
6	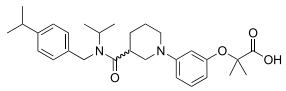	52 ± 9.3	46 ± 8.4
7	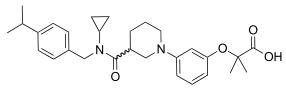	40 ± 8.5	36 ± 7.6

[a]The data were shown in the form of mean ± standard deviation (n = 3). [b]The K_i of **CP-868388** from the Sigma-Aldrich 90 LOPAC^{Pfizer} library was reported to be 1.2 ± 0.21 μM using the truncated β-catenin (residue 138−686).[50]

Table 2. AlphaScreen Assay Results of 8−15[a]

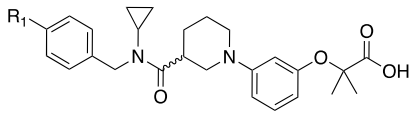

Compounds	R_1	IC_{50} ± SD (μM)	K_i ± SD (μM)	Compounds	R_1	IC_{50} ± SD (μM)	K_i ± SD (μM)
8		> 100	> 90	**12**		15 ± 4.4	13 ± 3.7
9		> 100	> 90	**13**		35 ± 3.9	30 ± 3.2
10		72 ± 1.5	61 ± 1.3	**14**		50 ± 4.5	42 ± 3.7
11		> 100	> 90	**15**		> 100	>90

[a]The data were shown as mean ± standard deviation (n = 3).

The results in Table 4 show for both compounds that the *S*-isomer (**28** and **30**) is slightly superior to the *R*-isomer (**27** and **29**).

Cell-Based Studies. The effects of **12**, **17**, **28**, and **30** on the viability of different cancer cells with hyperactive Wnt signaling were evaluated in MTS assays. The cell lines used include colorectal cancer HCT116 and SW480 cells and breast cancer MDA-MB-468 and MDA-MB-231 cells. The normal breast epithelial MCF10A cells were assessed in parallel for comparison. The results are shown in Table 5. The

https://doi.org/10.1021/acs.jmedchem.1c00046
J. Med. Chem. 2021, 64, 5886−5904

Table 3. AlphaScreen Assay Results of 16−26[a]

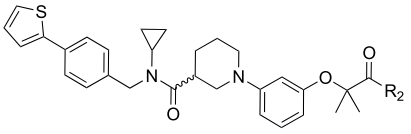

Compounds	R_2	$IC_{50} \pm SD$ (μM)	$K_i \pm SD$ (μM)	Compounds	R_2	$IC_{50} \pm SD$ (μM)	$K_i \pm SD$ (μM)
16	OMe	> 100	>90	**22**	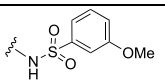	5.1 ± 0.43	4.1 ± 0.33
17	O*t*Bu	> 100	>90	**23**	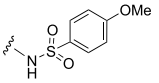	6.1 ± 0.38	4.9 ± 0.29
18		24 ± 2.7	21 ± 2.2	**24**	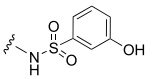	7.1 ± 0.53	5.8 ± 0.41
19	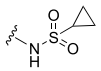	23 ± 3.0	19 ± 2.5	**25**	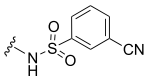	6.3 ± 0.27	5.1 ± 0.20
20	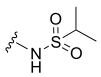	13 ± 0.71	11 ± 0.58	**26**	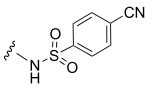	4.8 ± 0.26	3.9 ± 0.19
21	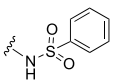	7.7 ± 0.67	6.4 ± 0.55				

[a]The data were shown as mean ± standard deviation (n = 3).

Table 4. AlphaScreen Assay Results of 27−30[a]

Compounds	Structure	$IC_{50} \pm SD$ (μM)	$K_i \pm SD$ (μM)
27	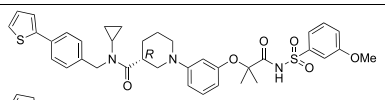	5.7 ± 0.19	4.6 ± 0.13
28	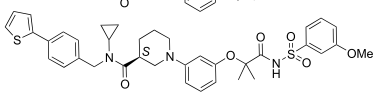	2.9 ± 0.34	2.3 ± 0.26
29	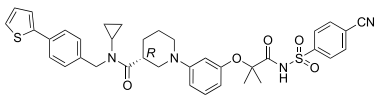	4.8 ± 0.67	3.9 ± 0.52
30	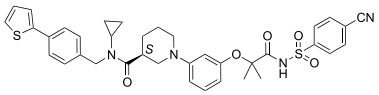	4.4 ± 0.27	3.6 ± 0.20

[a]The data were shown as mean ± standard deviation (n = 3).

Table 5. MTS Assay Results of 12, 17, 28, and 30 on Cell Viability[a]

	MTS $IC_{50} \pm SD$ (μM)				
	Wnt hyperactive				Wnt normal
compounds	SW480	HCT116	MDA-MB-231	MDA-MB-468	MCF10A
12	137 ± 8.20	112 ± 9.25	103 ± 7.44	95.9 ± 8.37	98.5 ± 7.66
17	>200	>200	>200	>200	>200
28	28.2 ± 1.08	29.9 ± 1.99	19.8 ± 1.59	15.4 ± 2.49	30.4 ± 2.47
30	16.3 ± 2.04	29.6 ± 1.02	14.3 ± 0.570	17.8 ± 1.01	139 ± 3.16

[a]The data were shown as mean ± standard deviation (n = 3).

https://doi.org/10.1021/acs.jmedchem.1c00046
J. Med. Chem. 2021, 64, 5886−5904

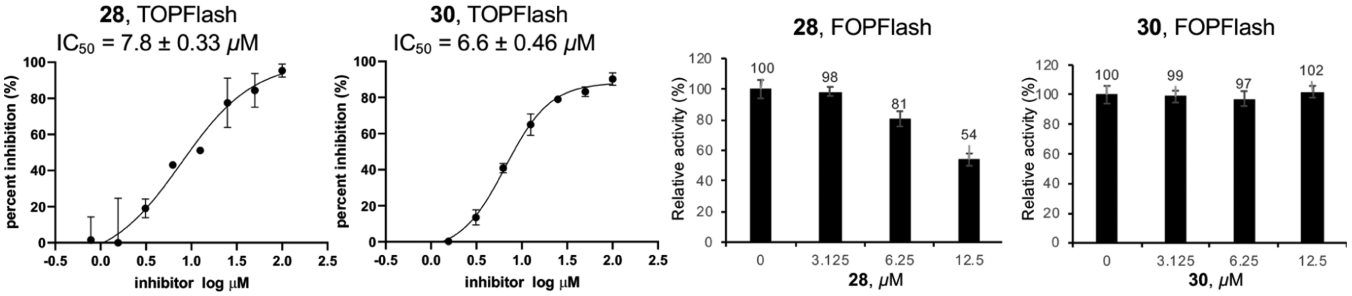

Figure 2. Wnt-dependent TOPFlash and FOPFlash experiment results of **28** and **30** in SW480 cells. Each experiment was performed in triplicate (n = 3).

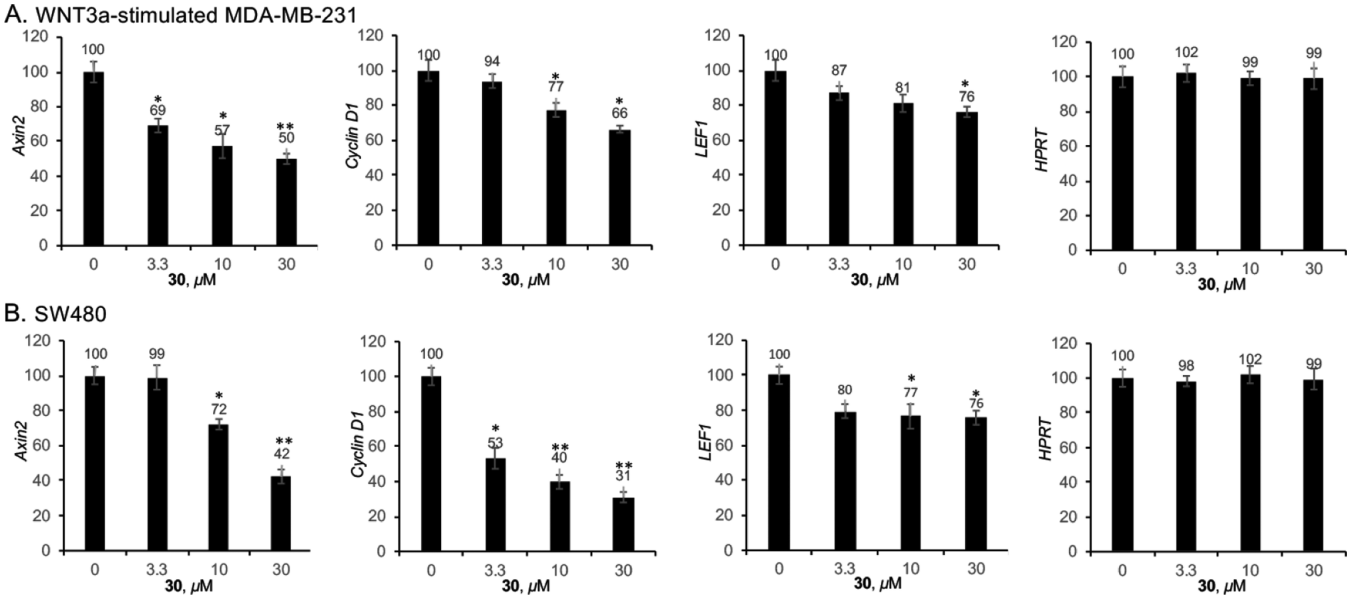

Figure 3. qPCR experiment results of *Axin2*, *cyclin D1*, and *LEF1* when treated with **30** (24-h incubation) in Wnt 3a-stimulated MDA-MB-231 (A) and SW480 cells (B). The negative control is the house-keeper gene *HPRT*. Each experiment was performed in triplicate (n = 3). *P < 0.05, **P < 0.01, as determined by Student t tests.

representative compound **30** inhibited the growth of Wnt hyperactive cancer cells with IC_{50}s between 14 and 30 μM, while sparing normal mammary epithelial MCF10A cells with 5- to 10-fold selectivity. Although **28** displayed similar IC_{50}s for Wnt hyperactive cancer cells, it was much less selective over MCF10A cells. In addition, an inactive analogue **17** in AlphaScreen assays (K_i > 90 μM, Table 3) did not show any inhibitory effects on all tested cells (IC_{50} > 200 μM, Table 5). One reason why **30** is more selective for Wnt-dependent breast cancer cells over normal mammary epithelial cells is perhaps because the CN derivative **30** is more hydrophilic than the OMe derivative **28**, and thus, **30** may have less-nonspecific off-target effects.

The inhibitory effects of **28** and **30** on transactivation of Wnt/β-catenin signaling were examined using the TOPFlash/FOPFlash luciferase reporter assay. For the TOPFlash assay, the reporter construct harbors three wild-type Tcf4 binding DNA sequences, while in the FOPFlash assay, Tcf4 binding sites were mutated. These tandem Tcf binding sites control the expression ratio of the firefly luciferase in TOPFlash/FOPFlash assays. The Renilla luciferase reporter construct (pCMV-RL) was used as the internal control to normalize luciferase reporter signals and eliminate any possible systematic errors. As shown in Figure 2, both **28** and **30** concentration-dependently suppressed the TOPFlash activity with the IC_{50} values of 7.8 and 6.6 μM, respectively. However, in this concentration range, compound **30** did not show any inhibition on the FOPFlash activity, indicating that **30** is specific for Wnt/β-catenin signaling. This selectivity trend is consistent with that from MTS cell viability assays. Therefore, further cell-based studies were focused on compound **30**.

Quantitative real-time PCR (qPCR) experiments were performed to evaluate the effects of **30** on transcription of the Wnt-specific target gene *Axin2* and two highly important oncogenic Wnt target genes, *LEF1* and *cyclin D1*. The results showed that **30** inhibited transcription of these Wnt target genes while sparing the house-keeper gene *HPRT* in both Wnt 3a-activated MDA-MB-231 and SW480 cells (Figure 3).

Western blot experiments were performed to determine the expression levels of the proteins Axin2 and cyclin D1. As shown in Figure 4A, treatment of **30** dose-dependently decreased the expression of both Axin2 and cyclin D1. To evaluate the binding of **30** to β-catenin in the cellular environment, we developed a protein pull-down assay using the *N*-terminally biotin-labeled BCL9 peptide (the homology domain 2 (HD2), residues 350–375) and the whole cell lysates of colorectal cancer SW480 cells. As shown in Figure 4B, β-catenin was pulled down by biotinylated BCL9, and the unlabeled BCL9 HD2 peptide served as a positive control to evaluate β-catenin/BCL9 disruption. Incubation of **30** resulted in the disruption of the

https://doi.org/10.1021/acs.jmedchem.1c00046
J. Med. Chem. 2021, 64, 5886–5904

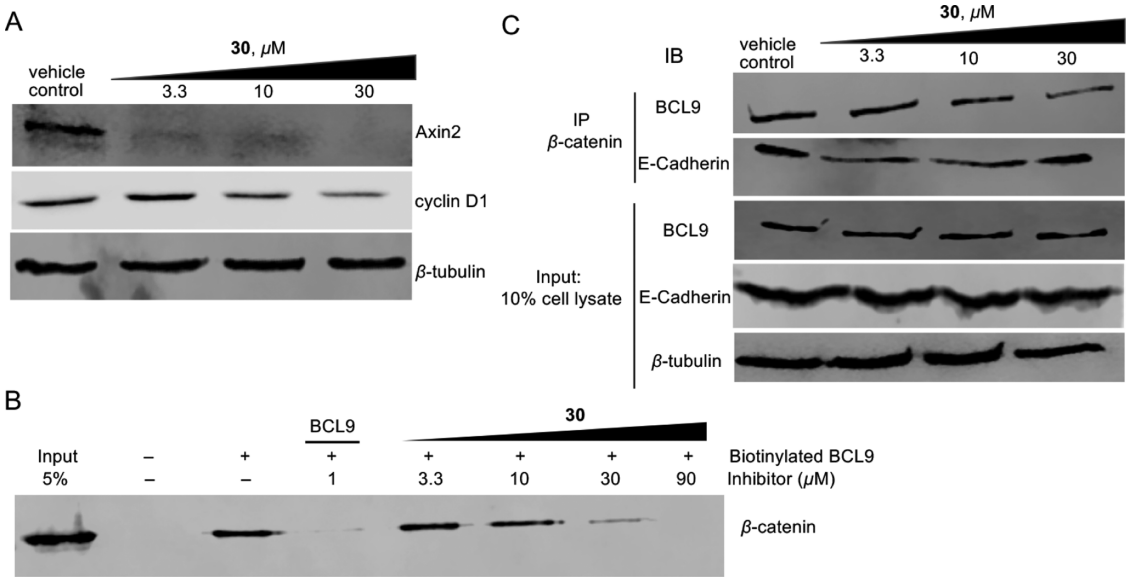

Figure 4. (A) Western blot results of Axin2 and cyclin D1 when treated with **30** (24 h incubation) in SW480 cells. The internal control is β-tubulin. The original Western blot images are provided in Figure S3. (B) Biotin−streptavidin endogenous β-catenin pulldown assay using SW480 cell lysates and the biotinylated BCL9 HD2 peptide (residues 350−375) after treatment with 1 μM BCL9 HD2 peptide (residues 350−375) and different concentrations of **30**. The original Western blot images are shown in Figure S4. (C) co-IP assays to examine the inhibitory effects **30** on β-catenin/BCL9 and β-catenin/E-cadherin interactions using HCT116 cells. The internal control is β-tubulin. IP, immunoprecipitation; IB, immunoblotting. Each experiment was conducted in triplicate. The original Western blot images are provided in Figure S5.

binding of β-catenin with biotinylated BCL9 in a dose-dependent manner, demonstrating that **30** can bind to the HD2 domain-binding groove of the endogenous β-catenin protein. Co-immunoprecipitation (co-IP) studies were further performed to examine effects of **30** on disruption of the full-length β-catenin/BCL9 interaction in cells. The results indicated that **30** concentration-dependently disrupted the β-catenin/BCL9 interaction (Figure 4C). Additional studies showed that **30** did not interfere with the β-catenin/E-cadherin interaction. This is important because the surface areas of β-catenin for β-catenin/BCL9 PPI are also used to bind E-cadherin region V, and the β-catenin/E-cadherin complex is critical for cell−cell adherens junctions.

To further evaluate cellular on-target effects of **30**, a β-catenin rescue experiment was performed following the recommendation by Dr. Kaelin.[54] Transfection with the empty pcDNA3.1 vector had no effect on the growth of SW480 cells. Compound **30** exhibits similar growth inhibition activities against SW480 cells with or without the empty pcDNA3.1 vector (IC_{50} = 19 μM vs 16 μM). As shown in Figure 5, the transfection of the constitutively active β-catenin rescued growth inhibition of compound **30**-treated SW480 cells, and the IC_{50} values of **30** were increased by fourfold after rescuing β-catenin. This rescue experiment, the β-catenin pull-down experiment using BCL9 HD2 peptide as the positive control (Figure 4B), the co-IP studies to examine disruption of cellular β-catenin-containing PPI complex structures (Figure 4C), and the TOPFlash/FOPFlash assays (Figure 2) demonstrated the cellular on-target effects of compound **30**.

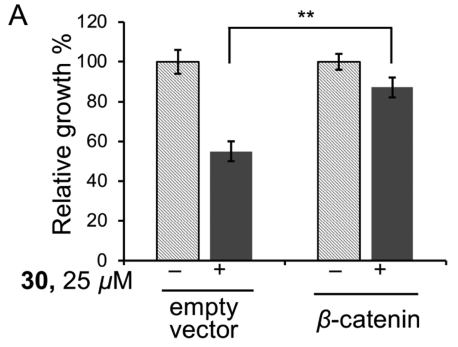

B

compound	IC_{50} ± SD (μM) empty vector	β-catenin
30	19 ± 0.86	86 ± 4.8

Figure 5. Results of β-catenin rescue experiments. The MTS assays were used to determine effects of **30** on growth inhibition of SW480 cells after 72 h treatment. The cells were transfected with a pcDNA3.1 empty vector or the pcDNA3.1−β-catenin vector. (A) Results when compound **30** was at the concentration of 25 μM. (B) IC_{50}s of **30** in MTS assays to inhibit the growth of SW480 cells that were transfected with pcDNA3.1 (empty vector) or pcDNA3.1−β-catenin. Each experiment was performed in triplicate (n = 3). The original dose−response curves are shown in Figure S6. **p < 0.01 calculated by Student t tests.

CHEMISTRY

The synthetic route for compounds **2**−**7** is shown in Scheme 1. The important intermediates **31** and **32a**−**c** were obtained through the nucleophilic substitution reaction and the reductive amination reaction using 4-isopropylbenzaldehyde and 3-bromophenol as starting materials, respectively. The newly prepared **32a**−**c** or other commercially available amines went through the amide coupling reaction with 1-Boc-piperidine-3-carboxylic acid to produce **33**. Removal of the Boc group of **33** and then Buchwald−Hartwig amination with **31** yielded compound **34**. The final products **2**−**7** were obtained by removing the *tert*-butyl group in **34** under acidic conditions.

The synthetic route for final products **8**−**15** is shown in Scheme 2. The intermediate **35** was synthesized through the reductive amination reaction using 4-bromobenzaldehyde and

https://doi.org/10.1021/acs.jmedchem.1c00046
J. Med. Chem. 2021, 64, 5886−5904

Scheme 1. Synthesis of Compounds 2−7

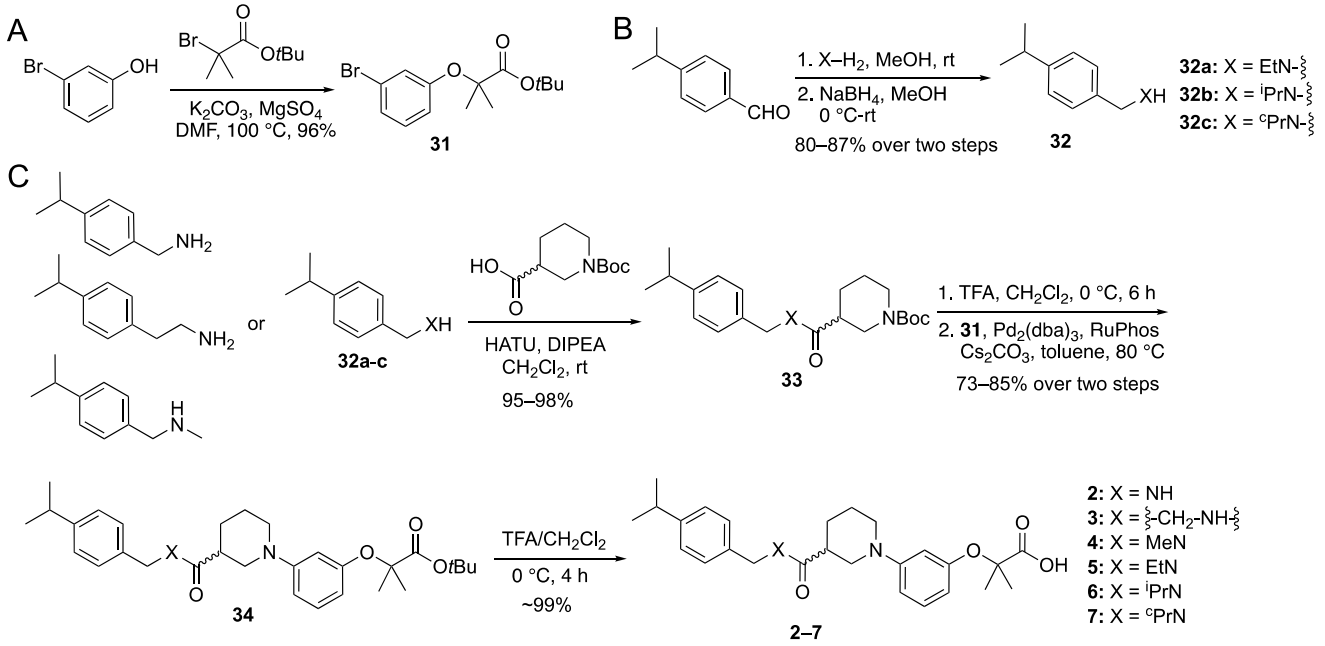

Scheme 2. Synthesis of Compounds 8−15

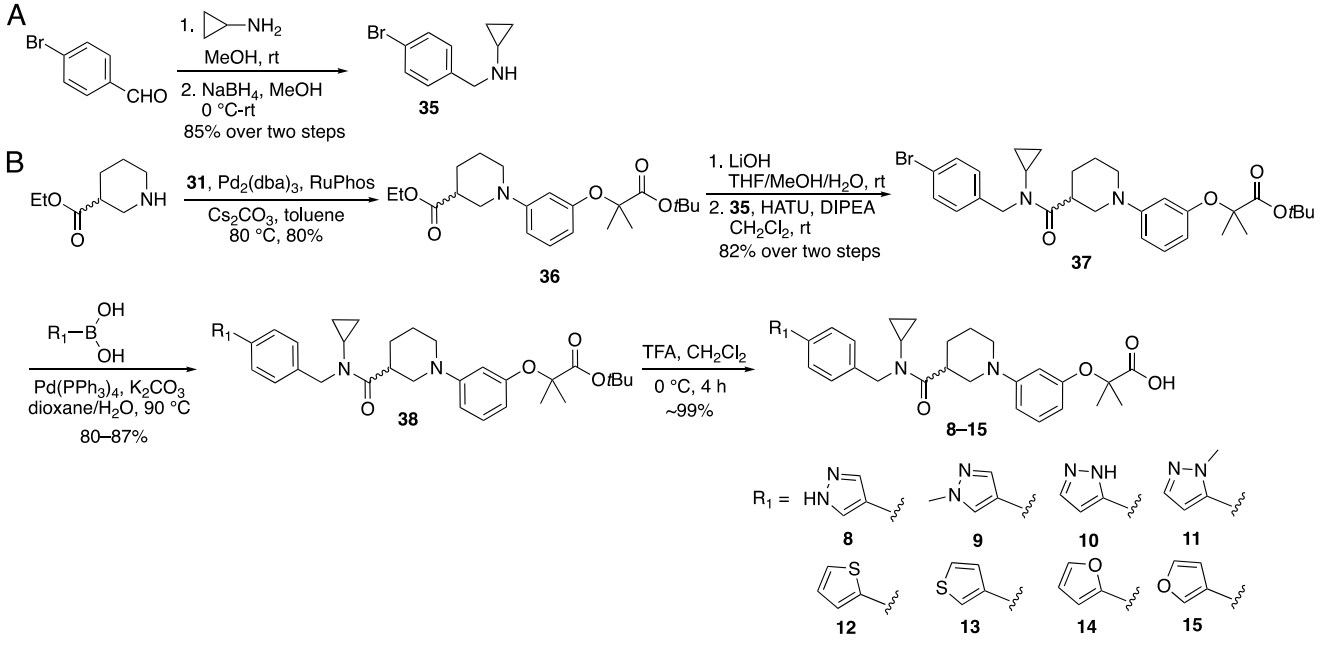

Scheme 3. Synthesis of Compounds 16−26

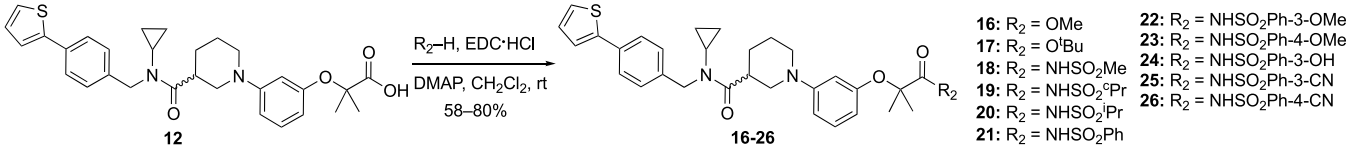

cyclopropylamine as the starting materials. Buchwald−Hartwig amination between ethyl piperidine-3-carboxylate and **31** yielded **36**. Hydrolysis of the ethyl ester in **36** and then amide coupling with **35** produced key intermediate **37**, which underwent Suzuki coupling with different boronic acids to generate **38**. Removal of the *tert*-butyl group in **38** with trifluoroacetic acid (TFA)/CH_2Cl_2 yielded final products **8**−**15**.

The synthetic route for final products **16**−**26** is shown in Scheme 3. Compounds **16** and **17** were obtained by the ester formation reactions between **12** and methanol or between **12** and *tert*-butanol, respectively. The other compounds (**18**−**26**)

https://doi.org/10.1021/acs.jmedchem.1c00046
J. Med. Chem. 2021, 64, 5886−5904

Scheme 4. Synthesis of Compounds 27 and 29

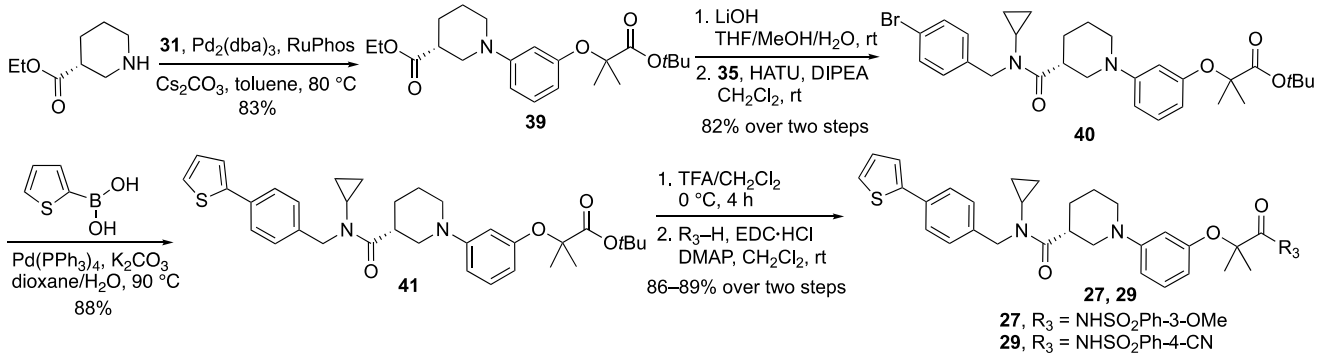

Scheme 5. Synthesis of Compounds 28 and 30

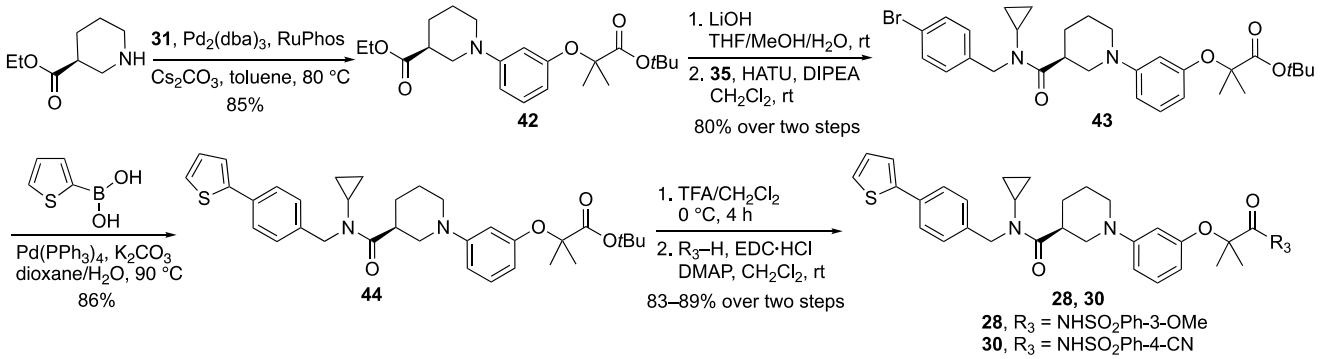

were achieved by the reactions between **12** and various sulfonamides.

The synthetic route for final products **27** and **29** is shown in Scheme 4. Ethyl (*R*)-piperidine-3-carboxylate underwent Buchwald−Hartwig amination with **31** yielded **39**. Hydrolysis of the ethyl ester in **39** and then amide coupling with **35** gave intermediate **40**. The Suzuki coupling reaction between **40** and thiophen-2-ylboronic acid produced **41**. Removing the *tert*-butyl group in **41** under acidic conditions and then reacting with 3-methoxybenzenesulfonamide and 4-cyanobenzenesulfonamide yielded final products **27** and **29**, respectively.

The synthetic route for final products **28** and **30** is shown in Scheme 5. Ethyl (*S*)-piperidine-3-carboxylate went through Buchwald−Hartwig amination with **31** to yield **42**. Hydrolysis of the ethyl ester in **42** and then amide coupling with **35** gave intermediate **43**, which underwent the Suzuki coupling reaction with thiophen-2-ylboronic acid to produce **44**. Final products **28** and **30** were obtained by removing the *tert*-butyl group in **44** and then reacting with 3-methoxybenzenesulfonamide or 4-cyanobenzenesulfonamide, respectively.

DISCUSSION AND CONCLUSIONS

Hyperactive Wnt/β-catenin signaling is frequently observed in various cancers. Targeting the downstream β-catenin-containing transcriptional complex, rather than the upstream effectors, appears to be the most effective approach for suppression of aberrant β-catenin signaling. However, targeting β-catenin to disrupt a β-catenin-related transcriptional complex is highly desirable but has proven to be a formidable challenge.[1,55,56] Most β-catenin-directed programs aimed at β-catenin/Tcf PPI, but very limited progress has been made. On one hand, the contacting area between β-catenin and Tcf is very large (3500 Å^2) and the binding constant (K_D) is 7−10 nM, suggesting that this PPI might be too difficult to be disrupted by small molecules.[57] β-Catenin interacts with Tcf, APC, and E-cadherin using the same surface areas, indicating that it would also be challenging to achieve high inhibitor selectivity.[57] On the other hand, BCL9 binds with β-catenin via a single α-helical structure (the HD2 domain).[57] β-Catenin and BCL9 have much smaller contacting interface areas (1450 Å^2), and their binding affinity is moderate (K_D = 0.47 μM). The only reported additional binding partner at this PPI area of β-catenin is E-cadherin. Therefore, the β-catenin/BCL9 PPI emerges as a promising alternative target to inhibit hyperactive Wnt/β-catenin signaling. In this work, structural optimization based on screening hit **1** (CP-868388) successfully yielded a series of novel selective β-catenin/BCL9 inhibitors. Co-IP studies show that the representative compound **30** not only disrupts β-catenin/BCL9 PPI in cells but also is selective for β-catenin/BCL9 over β-catenin/E-cadherin interactions.

This small-molecule β-catenin/BCL9 disruptor **30** we identified is structurally different from carnosic acid and PNPB series of β-catenin/BCL9 inhibitors and offers a new direction for future disruptor optimization. It is worth noting that both this series of inhibitors and carnosic acid contain an acidic functional group. In carnosic acid, it is a carboxylic acid group, while in **30**, it is a *N*-acyl sulfonamide group. The natural product scaffold of carnosic acid makes it difficult for further inhibitor optimization. The catechol group of carnosic acid has been identified as the pan-assay interference compound (PAINS) moiety. **PNPB-22** contains multiple aromatic rings and two positively charged centers (Figure 1). This lipophilic base character makes **PNPB-22** toxic to normal cells at high concentrations.[47] **PNPB-29** has two positively charged centers and one negatively charged center (Figure 1). This zwitterion has low cellular activity.[48] Compound **30** with a novel *N*-(2-(3-

https://doi.org/10.1021/acs.jmedchem.1c00046
J. Med. Chem. 2021, 64, 5886−5904

(3-carbamoylpiperidin-1-yl)phenoxy))acetyl sulfonamide scaffold displays low micromolar activity for disrupting the β-catenin/BCL9 interaction. This compound is PAINS-free, exhibits on-target cellular activities, and is ready for further optimization. This compound inhibits the viability of Wnt-dependent cancer cells and displays selectivity over normal breast epithelial MCF10A cells. Compared with the carboxylic acid (e.g., the original hit CP-868388), the additional substituent of *N*-acyl sulfonamide (in compound **30**) allows exploration of new binding space at the PPI interface while maintaining the necessary negative charge, resulting in a more potent inhibitor with desired cell-based activities. Indeed, the *N*-acyl sulfonamide moiety has been used to design PPI inhibitors.[53] ABT-199 (Venetoclax), a *N*-acyl sulfonamide-containing Bcl-2 PPI inhibitor was approved by FDA as a second-line treatment with chronic lymphocytic leukemia (CLL) with 17p deletion.[58,59] To reason why the racemic compound **26** displayed similar activities with its *R*-isomer **29** and *S*-isomer **30** in AlphaScreen assays, molecular modeling was carried out for **29** and **30**. The potential binding models of **29** and **30** with β-catenin are shown in Figure 6. For both **30** and **29**,

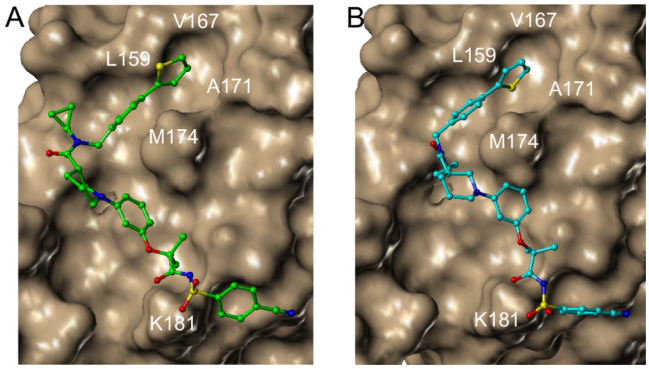

Figure 6. Docking models of **30** (A) and **29** (B) with the β-catenin armadillo repeat domain (PDB ID, 2GL7, residues 142−663). The limitation of this docking study was that the *N*-terminally disordered region (residues 1−141) of β-catenin was not observed in PDB ID 2GL7. If the *N*-terminally disordered region of β-catenin is involved in binding with these β-catenin/BCL9 inhibitors, these docking models might not be accurate.

the thiophene moiety can occupy the hydrophobic pocket surrounded by L159, V167, and A171 of β-catenin, while the *N*-acyl sulfonamide group was predicted to form polar interactions with K181.

In conclusion, the β-catenin/BCL9 interaction is an appealing therapeutic target to block hyperactive β-catenin signaling for cancer drug discovery. Our medicinal chemistry optimization on a screening hit successfully yielded novel small-molecule β-catenin/BCL9 disruptors. The representative compound **30** disrupts the β-catenin/BCL9 interaction with the K_i of 3.6 μM in AlphaScreen assays. It is noted that although the initial hit **1** inhibits the β-catenin/BCL9 interaction with a K_i of 11 μM in AlphaScreen assays, it does not show any cellular activity. Encouragingly, cell-based studies revealed that new inhibitor **30** disrupted β-catenin/BCL9 PPI, while sparing the β-catenin/E-cadherin complex, dose-dependently inhibited Wnt signaling transactivation, decreased the Wnt target gene expression, and selectively suppressed the growth of Wnt hyperactive cancer cells. This inhibitor with a novel scaffold can serve as a lead compound for further optimization of small-molecule disruptors of the β-catenin/BCL9 interaction.

EXPERIMENTAL SECTION

Chemical Synthesis. *General Methods, Reagents, and Materials.* All chemical reagents were obtained from commercial sources (Combi-Blocks, Inc.; Oakwood Products, Inc.; Fisher Scientific; and VWR International, LLC) and used without further purification. ^{1}H NMR and ^{13}C NMR spectra were collected on Bruker AVANCEIIIHD 500 (500 MHz) spectrometers (125.7 MHz for ^{13}C NMR spectra) in $CDCl_3$, DMSO-d_6, and d_4-methanol. Chemical shifts were reported as values in parts per million (ppm). The reference resonance peaks were set at 7.26 ppm ($CHCl_3$), 2.50 ppm [$(CD_2H)_2SO$], and 3.31 ppm (CD_2HOD) for ^{1}H NMR spectra and 77.23 ppm ($CDCl_3$), 39.52 ppm (DMSO-d_6), and 49.00 ppm (CD_3OD) for ^{13}C NMR spectra. High-resolution mass spectra were recorded using an Agilent G6230BA TOF LCMS mass spectrometer with a TOF mass detector. Low-resolution mass spectra were determined on an Agilent 6120 single quadrupole MS with 1220 infinity LC system (HPLC-MS) and an ESI source. Thin-layer chromatography was carried out on E. Merck pre-coated silica gel 60 F254 plates with a UV−visible lamp. Column chromatography was performed with SilicaFlash@ F60 (230−400 mesh). HPLC analyses were used to determine the purity of final compounds **2**−**30**. The instrument was an Agilent 1260 Infinity II HPLC system with a quaternary pump, a DAD detector, and a vial sampler. A Phenomenex C18 column (Luna 5 μL C18(2) 100 Å, 4.6 × 250 mm) was used in analytical HPLC analyses. The DAD detector was set to 254 nm. The purity of all tested compounds was determined to be >95%.

General Procedure for the Reductive Amination Reaction. A solution of aldehyde (1 mmol) and amine (2 mmol) in anhydrous methanol (5 mL) was stirred under Ar at room temperature overnight. $NaBH_4$ (1.5 mmol) was then added portion-wise to the reaction mixture at 0 °C. The mixture was stirred at 0 °C for 1 h. Saturated NH_4Cl was added, followed by the addition of ethyl acetate. The organic layer was collected and washed with brine, dried over anhydrous Na_2SO_4, concentrated under reduced pressure, and purified by column chromatography to yield the product.

General Procedure for the Amide Coupling Reaction. At 0 °C, to a mixture of carboxylic acid (1 mmol), amine (1.1 mmol), and HATU (1.5 mmol) in CH_2Cl_2 (10 mL) was added dropwise *N*,*N*-diisopropylethylamine (DIPEA) (2 mmol). The reaction mixture was warmed to room temperature and stirred overnight. After the reaction is completed, more CH_2Cl_2 was added, and the organic phase was washed with 1 M HCl, saturated $NaHCO_3$, and brine, dried over anhydrous Na_2SO_4, and concentrated in vacuo. Column chromatography was employed to purify the target compound.

General Procedure for Deprotection of Boc using 50% TFA in CH_2Cl_2. To a solution of Boc-protected amine (1 mmol) in 3 mL of CH_2Cl_2 was added TFA (3 mL) at room temperature. The reaction was then stirred for 3 h at room temperature. TFA was evaporated under the reduced pressure by adding CH_2Cl_2 three times to afford the desired product, which was used directly in the next step.

General procedure for the Buchwald−Hartwig amination Reaction. A solution of bromobenzene derivatives (1 mmol), amine (1.1 mmol), $Pd_2(dba)_3$ (0.1 mmol), RuPhos (0.2 mmol), and Cs_2CO_3 (2 mmol) in toluene (10 mL) was heated to 80 °C under argon and stirred overnight. The reaction mixture was cooled to room temperature. The solid was removed, and the filtrate was concentrated under reduced pressure and purified by column chromatography to yield the target compound.

General Procedure for Deprotection of tert-Butyl Using 50% TFA in CH_2Cl_2. At 0 °C, to a solution of *tert*-butyl ester (1 mmol) in CH_2Cl_2 (5 mL) was added TFA (5 mL) drop-wise. The reaction mixture was stirred at 0 °C for 6 h. Upon completion, the solvent was evaporated under the reduced pressure. TFA was removed by adding CH_2Cl_2 three times to afford the desired product, which was further purified by column chromatography.

General Procedure for Hydrolysis of Ethyl Ester. To a solution of ethyl ester (1 mmol) in THF (4 mL) and methanol (2 mL) was added a

https://doi.org/10.1021/acs.jmedchem.1c00046
J. Med. Chem. 2021, 64, 5886−5904

solution of LiOH (2 mmol) in H_2O (1 mL). The mixture was stirred at room temperature for 3 h. After the completion of the reaction, the solvent was removed under reduced pressure, and the residue was re-dissolved in H_2O and was acidified using 1 M HCl. Ethyl acetate was added, and the organic phase was washed with brine, dried over anhydrous Na_2SO_4, and concentrated under reduced pressure to yield the target compound, which was used directly in the next step.

General Procedure for the Suzuki Coupling Reaction. To a solution of bromobenzene derivatives (1 mmol) in dioxane/water (12/4 mL) were added boronic acid (1.2 mmol), $Pd(PPh_3)_4$ (0.1 mmol), and K_2CO_3 (2 mmol). The reaction mixture was heated to 90 °C under argon and stirred overnight. The reaction mixture was cooled to room temperature, concentrated under reduced pressure, then re-dissolved with ethyl acetate, washed with water and brine, and dried over Na_2SO_4. The solution obtained was concentrated under vacuum. The residue was purified by column chromatography to yield the target compound.

General Procedure for the Coupling Reaction between Carboxylic Acid and Alcohol or Sulfonamide. To a solution of carboxylic acid (1 mmol) and alcohol (1 mmol) or sulfonamide (1 mmol) in CH_2Cl_2 were added EDC·HCl (1.5 mmol) and DMAP (2 mmol). The mixture was stirred at room temperature overnight. More CH_2Cl_2 was added to the mixture, and the organic phase was washed with 1 M HCl and concentrated under reduced pressure. The pure compound was obtained by column chromatography.

Synthesis of tert-Butyl 2-(3-bromophenoxy)-2-methylpropanoate. A solution of 3-bromophenol (1 mmol), *tert*-butyl 2-bromo-2-methylpropanoate (5 mmol), K_2CO_3 (4 mmol), and $MgSO_4$ (1 mmol) in DMF was stirred at 100 °C overnight. The DMF was removed under reduced pressure. Water and ethyl acetate were added. The obtained organic layer was washed with brine, dried over Na_2SO_4, and concentrated under vacuum. The residue was purified by column chromatography to yield the target compound.

2-(3-(3-((4-Isopropylbenzyl)carbamoyl)piperidin-1-yl)-phenoxy)-2-methylpropanoic Acid (2). ^{1}H NMR (500 MHz, Chloroform-*d*): δ 7.30 (t, J = 5.9 Hz, 1H), 7.19 (t, J = 8.2 Hz, 1H), 7.14 (s, 4H), 7.08−6.96 (m, 2H), 6.84 (dd, J = 8.3, 2.1 Hz, 1H), 4.39 (dd, J = 14.7, 6.1 Hz, 1H), 4.24 (dd, J = 14.7, 5.4 Hz, 1H), 3.56−3.35 (m, 3H), 3.18 (dtd, J = 31.6, 12.0, 11.5, 3.5 Hz, 2H), 2.86 (hept, J = 6.9 Hz, 1H), 2.17−2.02 (m, 1H), 2.02−1.86 (m, 2H), 1.86−1.74 (m, 1H), 1.57 (s, 6H), 1.20 (d, J = 7.0 Hz, 6H). ^{13}C NMR (126 MHz, Chloroform-*d*): δ 175.9, 171.8, 156.8, 148.2, 144.3, 135.1, 130.7, 127.7, 126.7, 119.0, 113.4, 111.3, 79.8, 56.8, 55.4, 43.2, 41.0, 33.8, 25.4, 25.2, 25.1, 24.0, 22.5. HRMS (ESI): calcd for $C_{26}H_{34}N_2O_4$ (M − H)$^-$, 437.2446; found, 437.2443. HPLC purity 99.7%, t_R = 12.69 min.

2-(3-(3-((4-Isopropylphenethyl)carbamoyl)piperidin-1-yl)-phenoxy)-2-methylpropanoic Acid (3). ^{1}H NMR (500 MHz, Methanol-d_4): δ 7.35 (t, J = 8.2 Hz, 1H), 7.18−7.09 (m, 4H), 7.04 (dd, J = 8.2, 2.2 Hz, 1H), 6.99 (t, J = 2.3 Hz, 1H), 6.82 (dd, J = 8.3, 2.2 Hz, 1H), 3.56 (ddd, J = 15.9, 11.1, 4.3 Hz, 2H), 3.49 (dt, J = 14.1, 7.2 Hz, 1H), 3.45−3.33 (m, 2H), 3.31−3.20 (m, 1H), 2.81 (dt, J = 29.7, 6.9 Hz, 4H), 1.99−1.80 (m, 3H), 1.61 (s, 6H), 1.20 (dd, J = 6.9, 1.1 Hz, 6H). ^{13}C NMR (126 MHz, Methanol-d_4): δ 175.7, 173.7, 156.9, 146.8, 136.2, 130.2, 128.5, 126.0, 116.6, 112.8, 111.0, 79.3, 56.1, 53.7, 40.4, 34.6, 33.6, 25.7, 24.4, 24.3, 23.10, 23.12, 22.2. HRMS (ESI): calcd for $C_{27}H_{36}N_2O_4$ (M − H)$^-$, 451.2602; found, 451.2602. HPLC purity 98.0%, t_R = 12.76 min.

2-(3-(3-((4-Isopropylbenzyl)(methyl)carbamoyl)piperidin-1-yl)phenoxy)-2-methylpropanoic Acid (4). ^{1}H NMR (500 MHz, Chloroform-*d*): δ 9.01 (s, 2H), 7.26−7.19 (m, 2H), 7.19−7.12 (m, 2H), 7.11−7.08 (m, 2H), 7.08−6.98 (m, 1H), 6.86 (ddd, J = 26.7, 8.6, 1.9 Hz, 1H), 4.79−4.57 (m, 1H), 4.43 (dd, J = 20.4, 15.5 Hz, 1H), 3.70−3.44 (m, 4H), 3.20−2.95 (m, 4H), 2.88 (hept, J = 6.9 Hz, 1H), 2.28−1.67 (m, 4H), 1.65−1.55 (m, 6H), 1.23 (dd, J = 6.9, 2.0 Hz, 6H). ^{13}C NMR (126 MHz, Chloroform-*d*): δ 175.5, 172.7, 171.9, 156.8, 156.7, 148.6, 148.3, 144.8, 144.2, 133.7, 133.5, 130.8, 130.6, 127.9, 127.0, 126.8, 126.5, 119.6, 118.8, 113.6, 113.4, 111.8, 111.5, 80.0, 56.5, 56.2, 55.8, 55.2, 53.3, 50.9, 37.2, 37.0, 34.8, 33.79, 33.76, 25.9, 25.35, 25.30, 25.26, 25.01, 24.97, 24.0, 23.9, 22.7. HRMS (ESI): calcd for $C_{27}H_{36}N_2O_4$ (M − H)$^-$, 451.2602; found, 451.2599. HPLC purity 99.1%, t_R = 12.99 min.

2-(3-(3-(Ethyl(4-isopropylbenzyl)carbamoyl)piperidin-1-yl)-phenoxy)-2-methylpropanoic Acid (5). ^{1}H NMR (500 MHz, Chloroform-*d*): δ 7.30−7.18 (m, 3H), 7.16 (d, J = 8.1 Hz, 1H), 7.13−7.01 (m, 3H), 6.87 (ddd, J = 23.2, 8.2, 2.2 Hz, 1H), 4.66 (dd, J = 40.0, 15.8 Hz, 1H), 4.45 (t, J = 15.0 Hz, 1H), 3.78−3.21 (m, 6H), 3.20−2.96 (m, 1H), 2.94−2.81 (m, 1H), 2.45−1.64 (m, 4H), 1.60 (t, J = 2.7 Hz, 6H), 1.22 (dd, J = 6.9, 3.3 Hz, 6H), 1.17 (t, J = 7.1 Hz, 2H), 1.10 (t, J = 7.1 Hz, 1H). ^{13}C NMR (126 MHz, Chloroform-*d*): δ 175.3, 172.2, 171.8, 162.3, 162.0, 156.8, 156.6, 148.6, 148.2, 144.1, 134.3, 133.9, 130.8, 130.6, 127.8, 127.0, 126.7, 126.5, 119.9, 119.2, 113.7, 113.5, 112.1, 111.8, 80.1, 80.0, 56.6, 56.4, 55.9, 55.3, 50.6, 47.9, 41.94, 41.87, 37.4, 36.9, 33.78, 33.76, 26.1, 25.8, 25.3, 24.9, 24.0, 23.9, 22.73, 22.68, 14.1, 12.6. HRMS (ESI): calcd for $C_{28}H_{38}N_2O_4$ (M − H)$^-$, 465.2759; found, 465.2758. HPLC purity 98.9%, t_R = 13.27 min.

2-(3-(3-(Isopropyl(4-isopropylbenzyl)carbamoyl)piperidin-1-yl)phenoxy)-2-methylpropanoic Acid (6). ^{1}H NMR (500 MHz, Chloroform-*d*): δ 7.28−7.08 (m, 5H), 7.06 (d, J = 8.2 Hz, 1H), 7.02−6.91 (m, 1H), 6.91−6.75 (m, 1H), 4.80 (p, J = 6.8 Hz, 0.5H), 4.58 (t, J = 16.0 Hz, 1H), 4.40 (t, J = 16.8 Hz, 1H), 4.24 (p, J = 6.6 Hz, 0.5H), 3.62 (d, J = 29.3 Hz, 2H), 3.50 (t, J = 14.6 Hz, 1H), 3.38 (t, J = 11.5 Hz, 0.5H), 3.14 (dd, J = 13.2, 10.1 Hz, 1H), 2.96 (td, J = 11.6, 4.4 Hz, 0.5H), 2.87 (dp, J = 13.9, 6.9 Hz, 1H), 2.25 (t, J = 13.6 Hz, 0.5H), 2.10−1.90 (m, 1H), 1.85−1.38 (m, 8.5H), 1.31−0.82 (m, 12H). ^{13}C NMR (126 MHz, Chloroform-*d*): δ 175.2, 173.2, 156.7, 156.5, 148.2, 147.3, 136.0, 135.3, 130.7, 130.5, 126.8, 126.49, 126.47, 126.2, 113.7, 113.4, 112.1, 111.6, 80.2, 80.0, 56.5, 56.1, 55.8, 54.8, 49.2, 46.4, 46.1, 43.9, 38.7, 37.3, 33.70, 33.68, 26.3, 25.8, 25.24, 25.18, 25.0, 24.9, 24.0, 23.9, 22.9, 22.7, 21.8, 21.7, 20.5, 20.2. HRMS (ESI): calcd for $C_{29}H_{40}N_2O_4$ (M − H)$^-$, 479.2915; found, 479.2914. HPLC purity 100%, t_R = 13.70 min.

(*R*)-2-(3-(3-(Cyclopropyl(4-isopropylbenzyl)carbamoyl)-piperidin-1-yl)phenoxy)-2-methylpropanoic Acid (7). ^{1}H NMR (500 MHz, Chloroform-*d*): δ 7.34−7.22 (m, 1H), 7.22−7.02 (m, 6H), 6.90 (dd, J = 8.3, 2.2 Hz, 1H), 4.69 (d, J = 14.6 Hz, 1H), 4.44 (d, J = 14.4 Hz, 1H), 4.06 (dd, J = 13.3, 9.6 Hz, 1H), 3.80−3.46 (m, 3H), 3.14 (td, J = 12.5, 3.1 Hz, 1H), 2.89 (p, J = 6.9 Hz, 1H), 2.66 (tt, J = 6.8, 4.1 Hz, 1H), 2.24 (q, J = 13.6 Hz, 1H), 2.13−1.93 (m, 2H), 1.77 (qd, J = 13.1, 3.8 Hz, 1H), 1.62 (s, 6H), 1.25 (d, J = 6.9 Hz, 6H), 1.13−0.36 (m, 4H). ^{13}C NMR (126 MHz, Chloroform-*d*): δ 175.4, 174.7, 156.7, 147.9, 144.5, 134.9, 130.7, 127.5, 126.7, 119.6, 113.5, 111.8, 80.0, 56.1, 55.8, 49.9, 37.9, 33.8, 30.0, 25.6, 25.3, 24.9, 24.0, 22.9, 9.5, 8.7. HRMS (ESI): calcd for $C_{29}H_{38}N_2O_4$ (M − H)$^-$, 477.2759; found, 477.2753. HPLC purity 97.9%, t_R = 13.45 min.

2-(3-(3-((4-(1*H*-Pyrazol-4-yl)benzyl)(cyclopropyl)-carbamoyl)piperidin-1-yl)phenoxy)-2-methylpropanoic Acid (8). ^{1}H NMR (500 MHz, DMSO-d_6): δ 8.02 (s, 2H), 7.55 (d, J = 8.1 Hz, 2H), 7.16 (dd, J = 7.9, 5.9 Hz, 3H), 6.73 (s, 1H), 6.56 (s, 1H), 6.34 (s, 1H), 4.63 (d, J = 15.0 Hz, 1H), 4.40 (d, J = 15.0 Hz, 1H), 3.76−3.67 (m, 1H), 3.65 (d, J = 12.4 Hz, 1H), 3.48 (s, 1H), 2.92 (d, J = 52.1 Hz, 2H), 2.70 (tt, J = 6.8, 4.1 Hz, 1H), 1.94 (d, J = 11.3 Hz, 1H), 1.79 (d, J = 13.0 Hz, 1H), 1.70−1.57 (m, 2H), 1.49 (d, J = 3.1 Hz, 6H), 0.90−0.75 (m, 4H). ^{13}C NMR (126 MHz, DMSO-d_6): δ 175.6, 156.7, 136.5, 132.0, 131.2, 130.1, 128.0, 125.7, 121.4, 78.8, 53.0, 49.0, 38.9, 29.9, 27.4, 25.6, 25.5, 23.9, 9.5, 8.7. HRMS (ESI): calcd for $C_{29}H_{34}N_4O_4$ (M − H)$^-$, 501.2507; found, 501.2512. HPLC purity 99.1%, t_R = 10.83 min.

2-(3-(3-(Cyclopropyl(4-(1-methyl-1*H*-pyrazol-4-yl)benzyl)-carbamoyl)piperidin-1-yl)phenoxy)-2-methylpropanoic Acid (9). ^{1}H NMR (500 MHz, Chloroform-*d*): δ 7.52 (d, J = 2.0 Hz, 1H), 7.39−7.32 (m, 2H), 7.29 (d, J = 8.1 Hz, 2H), 7.09 (t, J = 8.2 Hz, 1H), 6.63 (dd, J = 8.2, 2.2 Hz, 1H), 6.60 (s, 1H), 6.41 (dd, J = 8.1, 2.2 Hz, 1H), 6.29 (d, J = 1.9 Hz, 1H), 4.70 (d, J = 14.9 Hz, 1H), 4.59 (d, J = 14.9 Hz, 1H), 3.87 (s, 3H), 3.65 (dd, J = 12.7, 3.5 Hz, 2H), 3.49 (s, 1H), 3.00 (t, J = 11.6 Hz, 1H), 2.81−2.70 (m, 1H), 2.66 (tt, J = 7.0, 4.0 Hz, 1H), 1.96 (d, J = 8.0 Hz, 1H), 1.87−1.67 (m, 3H), 1.59 (s, 6H), 0.96−0.78 (m, 4H). ^{13}C NMR (126 MHz, Chloroform-*d*): δ 177.1, 176.6, 155.8, 152.3, 143.4, 138.8, 138.4, 129.5, 129.3, 128.9, 127.8, 111.4, 111.0, 108.9, 106.0, 79.5, 52.3, 50.4, 49.8, 39.8, 37.4, 30.1, 27.7, 25.3, 25.1, 24.4, 9.5, 9.1. HRMS (ESI): calcd for $C_{30}H_{36}N_4O_4$ (M − H)$^-$, 515.2664; found, 515.2673. HPLC purity 99.5%, t_R = 11.58 min.

2-(3-(3-((4-(1*H*-Pyrazol-5-yl)benzyl)(cyclopropyl)-carbamoyl)piperidin-1-yl)phenoxy)-2-methylpropanoic Acid (10). ^{1}H NMR (500 MHz, DMSO-d_6): δ 7.74 (d, J = 8.1 Hz, 2H),

https://doi.org/10.1021/acs.jmedchem.1c00046
J. Med. Chem. 2021, 64, 5886−5904

7.70 (d, J = 2.2 Hz, 1H), 7.22 (d, J = 8.0 Hz, 2H), 7.14 (t, J = 8.2 Hz, 1H), 6.78−6.63 (m, 2H), 6.55 (s, 1H), 6.33 (d, J = 8.1 Hz, 1H), 4.65 (d, J = 15.2 Hz, 1H), 4.44 (d, J = 15.1 Hz, 1H), 3.78−3.69 (m, 1H), 3.65 (d, J = 11.9 Hz, 1H), 3.47 (s, 1H), 2.91 (d, J = 53.2 Hz, 2H), 2.73 (tt, J = 6.9, 4.1 Hz, 1H), 1.95 (d, J = 11.1 Hz, 1H), 1.84−1.56 (m, 3H), 1.49 (d, J = 3.1 Hz, 6H), 0.92−0.70 (m, 4H). ^{13}C NMR (126 MHz, DMSO-d_6): δ 176.0, 175.6, 156.7, 138.2, 133.2, 131.6, 130.1, 127.9, 125.7, 110.7, 107.8, 102.3, 78.7, 52.8, 50.4, 49.1, 38.9, 30.0, 27.4, 25.6, 25.5, 24.0, 9.5, 8.7. HRMS (ESI): calcd for $C_{29}H_{34}N_4O_4$ (M − H)$^-$, 501.2507; found, 501.2511. HPLC purity 99.5%, t_R = 10.91 min.

2-(3-(3-(Cyclopropyl(4-(1-methyl-1*H*-pyrazol-5-yl)benzyl)carbamoyl)piperidin-1-yl)phenoxy)-2-methylpropanoic Acid (11). ^{1}H NMR (500 MHz, Chloroform-d): δ 7.79−7.72 (m, 1H), 7.58 (s, 1H), 7.46−7.36 (m, 2H), 7.20 (d, J = 7.9 Hz, 2H), 7.09 (t, J = 8.2 Hz, 1H), 6.63 (dd, J = 8.2, 2.2 Hz, 1H), 6.56 (t, J = 2.3 Hz, 1H), 6.45−6.35 (m, 1H), 4.67 (d, J = 14.6 Hz, 1H), 4.51 (d, J = 14.6 Hz, 1H), 3.93 (s, 3H), 3.64 (t, J = 8.4 Hz, 2H), 3.46 (s, 1H), 2.99 (t, J = 11.6 Hz, 1H), 2.79−2.69 (m, 1H), 2.58 (tt, J = 6.8, 4.0 Hz, 1H), 1.93 (d, J = 7.9 Hz, 1H), 1.86−1.68 (m, 3H), 1.58 (s, 6H), 0.91−0.76 (m, 4H). ^{13}C NMR (126 MHz, Chloroform-d): δ 176.9, 176.6, 155.6, 152.3, 136.6, 136.4, 131.4, 129.5, 128.3, 127.0, 125.7, 122.9, 111.5, 111.1, 109.1, 79.6, 52.3, 50.4, 49.6, 39.8, 39.0, 29.8, 27.6, 25.2, 25.1, 24.4, 9.5, 9.0. HRMS (ESI): calcd for $C_{30}H_{36}N_4O_4$ (M − H)$^-$, 515.2664; found, 515.2674. HPLC purity 99.8%, t_R = 11.57 min.

2-(3-(3-(Cyclopropyl(4-(thiophen-2-yl)benzyl)carbamoyl)-piperidin-1-yl)phenoxy)-2-methylpropanoic Acid (12). ^{1}H NMR (500 MHz, Chloroform-d): δ 7.50−7.45 (m, 2H), 7.21 (dd, J = 3.6, 1.2 Hz, 1H), 7.19−7.17 (m, 1H), 7.14 (d, J = 8.0 Hz, 2H), 7.02−6.97 (m, 2H), 6.56 (dd, J = 8.2, 2.3 Hz, 1H), 6.50 (d, J = 2.4 Hz, 1H), 6.33 (dd, J = 8.1, 2.3 Hz, 1H), 4.64 (d, J = 14.7 Hz, 1H), 4.42 (d, J = 14.7 Hz, 1H), 3.56 (d, J = 11.6 Hz, 2H), 3.41 (tt, J = 11.4, 3.6 Hz, 1H), 2.93 (t, J = 11.6 Hz, 1H), 2.65 (td, J = 11.9, 3.3 Hz, 1H), 2.51 (tt, J = 6.9, 4.0 Hz, 1H), 1.85 (d, J = 7.8 Hz, 1H), 1.74−1.62 (m, 3H), 1.50 (s, 6H), 0.83−0.71 (m, 4H). ^{13}C NMR (126 MHz, Chloroform-d): δ 177.2, 177.1, 155.8, 152.1, 144.1, 137.5, 133.4, 129.5, 128.3, 128.0, 126.1, 124.7, 123.0, 111.5, 111.2, 109.1, 79.4, 52.4 50.6, 49.6, 39.7, 29.9, 27.6, 25.3, 25.2, 24.3, 9.6, 9.0. HRMS (ESI): calcd for $C_{30}H_{34}N_2O_4S$ (M − H)$^-$, 517.2167; found, 517.2176. HPLC purity 99.2%, t_R = 13.56 min.

2-(3-(3-(Cyclopropyl(4-(thiophen-3-yl)benzyl)carbamoyl)-piperidin-1-yl)phenoxy)-2-methylpropanoic Acid (13). ^{1}H NMR (500 MHz, Chloroform-d): δ 7.48−7.44 (m, 2H), 7.35 (t, J = 2.2 Hz, 1H), 7.29 (d, J = 2.1 Hz, 2H), 7.18−7.15 (m, 2H), 7.00 (t, J = 8.2 Hz, 1H), 6.56 (dd, J = 8.2, 2.3 Hz, 1H), 6.51 (t, J = 2.4 Hz, 1H), 6.33 (dd, J = 8.1, 2.2 Hz, 1H), 4.64 (d, J = 14.7 Hz, 1H), 4.44 (d, J = 14.6 Hz, 1H), 3.61−3.51 (m, 2H), 3.42 (ddd, J = 11.2, 7.4, 3.5 Hz, 1H), 2.98−2.89 (m, 1H), 2.65 (td, J = 11.8, 3.4 Hz, 1H), 2.51 (tt, J = 6.9, 4.1 Hz, 1H), 1.86 (d, J = 7.8 Hz, 1H), 1.74−1.62 (m, 3H), 1.50 (s, 6H), 0.82−0.70 (m, 4H). ^{13}C NMR (126 MHz, Chloroform-d): δ 177.1, 177.0, 155.8, 152.1, 141.9, 137.1, 134.8, 129.5, 128.2, 126.6, 126.2, 120.2, 111.5, 111.2, 109.1, 79.4, 52.4, 50.6, 49.6, 39.7, 29.9, 27.5, 25.3, 25.2, 24.3, 9.5, 9.0. HRMS (ESI): calcd for $C_{30}H_{34}N_2O_4S$ (M − H)$^-$, 517.2167; found, 517.2170. HPLC purity 99.9%, t_R = 13.43 min.

2-(3-(3-(Cyclopropyl(4-(furan-2-yl)benzyl)carbamoyl)-piperidin-1-yl)phenoxy)-2-methylpropanoic Acid (14). ^{1}H NMR (500 MHz, Chloroform-d): δ 7.64−7.58 (m, 2H), 7.45 (d, J = 1.7 Hz, 1H), 7.24 (d, J = 8.1 Hz, 2H), 7.12−7.07 (m, 1H), 6.64 (dd, J = 12.7, 5.9 Hz, 2H), 6.57 (t, J = 2.4 Hz, 1H), 6.46 (dd, J = 3.3, 1.8 Hz, 1H), 6.41 (dd, J = 8.1, 2.2 Hz, 1H), 4.72 (d, J = 14.6 Hz, 1H), 4.49 (d, J = 14.7 Hz, 1H), 3.70−3.60 (m, 2H), 3.48 (s, 1H), 3.01 (t, J = 11.6 Hz, 1H), 2.73 (dt, J = 11.9, 6.3 Hz, 1H), 2.58 (tt, J = 6.6, 4.0 Hz, 1H), 1.94 (d, J = 8.5 Hz, 1H), 1.82−1.70 (m, 3H), 1.58 (s, 6H), 0.89−0.78 (m, 4H). ^{13}C NMR (126 MHz, Chloroform-d): δ 177.0, 155.6, 153.7, 152.2, 142.0, 137.3, 129.9, 129.5, 128.1, 124.0, 113.9, 111.4, 109.2, 104.9, 79.6, 52.3, 50.5, 49.6, 39.7, 29.8, 27.6, 25.2, 25.1, 24.4, 9.6, 9.0. HRMS (ESI): calcd for $C_{30}H_{34}N_2O_5$ (M − H)$^-$, 501.2395; found, 501.2405. HPLC purity 96.0%, t_R = 13.22 min.

2-(3-(3-(Cyclopropyl(4-(furan-3-yl)benzyl)carbamoyl)-piperidin-1-yl)phenoxy)-2-methylpropanoic Acid (15). ^{1}H NMR (500 MHz, Chloroform-d): δ 7.71 (t, J = 1.2 Hz, 1H), 7.46 (t, J = 1.7 Hz, 3H), 7.22 (d, J = 8.0 Hz, 2H), 7.09 (t, J = 8.2 Hz, 1H), 6.72−6.62 (m, 2H), 6.58 (t, J = 2.4 Hz, 1H), 6.41 (dd, J = 8.0, 2.2 Hz, 1H), 4.71 (d, J = 14.7 Hz, 1H), 4.50 (d, J = 14.6 Hz, 1H), 3.70−3.57 (m, 2H), 3.48 (d, J = 11.0 Hz, 1H), 3.01 (t, J = 11.7 Hz, 1H), 2.74 (td, J = 12.1, 11.6, 3.4 Hz, 1H), 2.58 (ddt, J = 9.6, 6.8, 4.0 Hz, 1H), 1.94 (d, J = 8.6 Hz, 1H), 1.84−1.70 (m, 3H), 1.58 (s, 6H), 0.90−0.77 (m, 4H). ^{13}C NMR (126 MHz, Chloroform-d): δ 177.0, 176.8, 155.6, 152.1, 143.7, 138.4, 137.0, 131.3, 129.5, 128.2, 126.1, 126.0, 111.7, 111.4, 109.2, 108.8, 79.6, 52.3, 50.5, 49.6, 39.7, 29.8, 27.6, 25.2, 25.1, 24.4, 9.5, 9.0. HRMS (ESI): calcd for $C_{30}H_{34}N_2O_5$ (M − H)$^-$, 501.2395; found, 501.2404. HPLC purity 98.8%, t_R = 13.06 min.

Methyl 2-(3-(3-(cyclopropyl(4-(thiophen-2-yl)benzyl)-carbamoyl)piperidin-1-yl)phenoxy)-2-methylpropanoate (16). ^{1}H NMR (500 MHz, Chloroform-d): δ 7.58−7.53 (m, 2H), 7.29−7.24 (m, 4H), 7.09−7.04 (m, 2H), 6.64−6.54 (m, 1H), 6.48 (s, 1H), 6.25 (dd, J = 8.2, 2.2 Hz, 1H), 4.67 (d, J = 14.7 Hz, 1H), 4.57 (d, J = 14.8 Hz, 1H), 3.74 (s, 3H), 3.71−3.66 (m, 2H), 3.45 (s, 1H), 3.01 (t, J = 11.7 Hz, 1H), 2.82−2.74 (m, 1H), 2.61 (ddt, J = 10.8, 6.9, 4.0 Hz, 1H), 2.01−1.93 (m, 1H), 1.77 (ddd, J = 20.6, 17.2, 8.3 Hz, 3H), 1.58 (s, 6H), 0.91−0.82 (m, 4H). ^{13}C NMR (126 MHz, Chloroform-d): δ 176.8, 175.0, 156.4, 144.1, 137.7, 133.3, 129.4, 128.3, 128.0, 126.1, 124.7, 123.0, 110.7, 109.3, 107.9, 78.9, 52.5, 52.3, 50.1, 49.5, 39.8, 29.8, 27.8, 25.5, 25.4, 24.4, 9.5, 9.1. HRMS (ESI): calcd for $C_{31}H_{36}N_2O_4S$ (M + H)$^+$ 533.2469; found, 533.2469. HPLC purity 99.0%, t_R = 14.44 min.

***tert*-Butyl 2-(3-(3-(cyclopropyl(4-(thiophen-2-yl)benzyl)-carbamoyl)piperidin-1-yl)phenoxy)-2-methylpropanoate (17).** ^{1}H NMR (500 MHz, Chloroform-d): δ 7.53−7.42 (m, 2H), 7.24−7.12 (m, 4H), 7.04−6.93 (m, 2H), 6.48 (dd, J = 8.2, 2.3 Hz, 1H), 6.41 (t, J = 2.3 Hz, 1H), 6.22 (dd, J = 8.1, 2.3 Hz, 1H), 4.59 (d, J = 14.7 Hz, 1H), 4.48 (d, J = 14.7 Hz, 1H), 3.69−3.51 (m, 2H), 3.37 (tt, J = 10.9, 3.0 Hz, 1H), 2.99−2.82 (m, 1H), 2.70 (td, J = 12.2, 2.8 Hz, 1H), 2.59−2.44 (m, 1H), 1.86 (d, J = 11.3 Hz, 1H), 1.75−1.63 (m, 3H), 1.47 (s, 6H), 1.35 (s, 9H), 0.85−0.66 (m, 4H). ^{13}C NMR (126 MHz, Chloroform-d): δ 176.9, 173.5, 156.7, 152.4, 144.1, 137.7, 133.3, 129.2, 128.3, 128.0, 126.1, 124.7, 123.0, 110.2, 109.1, 107.6, 81.5, 79.2, 52.2, 50.0, 49.5, 39.8, 29.8, 27.9, 27.8, 25.53, 25.47, 24.5, 9.5, 9.1. HRMS (ESI): calcd for $C_{34}H_{42}N_2O_4S$ (M + H)$^+$ 575.2938; found, 575.2925. HPLC purity 100%, t_R = 15.31 min.

***N*-Cyclopropyl-1-(3-((2-methyl-1-(methylsulfonamido)-1-oxopropan-2-yl)oxy)phenyl)-*N*-(4-(thiophen-2-yl)benzyl)-piperidine-3-carboxamide (18).** ^{1}H NMR (500 MHz, Chloroform-d): δ 8.93 (s, 1H), 7.52−7.45 (m, 2H), 7.22 (dd, J = 3.6, 1.2 Hz, 1H), 7.20−7.16 (m, 3H), 7.08 (t, J = 8.2 Hz, 1H), 7.00 (dd, J = 5.1, 3.5 Hz, 1H), 6.70−6.56 (m, 1H), 6.41 (t, J = 2.4 Hz, 1H), 6.28 (dd, J = 8.2, 2.2 Hz, 1H), 4.67 (d, J = 14.7 Hz, 1H), 4.43 (d, J = 14.7 Hz, 1H), 3.68−3.55 (m, 2H), 3.43−3.30 (m, 1H), 3.25 (s, 3H), 2.97 (t, J = 11.6 Hz, 1H), 2.73 (t, J = 10.6 Hz, 1H), 2.55 (tt, J = 7.0, 4.1 Hz, 1H), 1.91 (d, J = 9.8 Hz, 1H), 1.81−1.75 (m, 1H), 1.72−1.63 (m, 2H), 1.47 (s, 6H), 0.86−0.74 (m, 4H). ^{13}C NMR (126 MHz, Chloroform-d): δ 176.8, 174.2, 154.1, 152.7, 144.1, 137.6, 133.3, 129.7, 128.3, 128.0, 126.1, 124.7, 123.0, 112.3, 111.5, 109.8, 81.5, 51.9, 49.9, 49.5, 41.3, 39.8, 29.8, 27.8, 24.6, 24.5, 9.6, 9.0. HRMS (ESI): calcd for $C_{31}H_{37}N_3O_5S_2$ (M − H)$^-$, 594.2102; found, 594.2107. HPLC purity 97.3%, t_R = 13.86 min.

1-(3-((1-(Cyclopropanesulfonamido)-2-methyl-1-oxopropan-2-yl)oxy)phenyl)-*N*-cyclopropyl-*N*-(4-(thiophen-2-yl)-benzyl)piperidine-3-carboxamide (19). ^{1}H NMR (500 MHz, Chloroform-d): δ 8.87 (s, 1H), 7.52−7.46 (m, 2H), 7.23−7.16 (m, 4H), 7.07 (t, J = 8.2 Hz, 1H), 7.00 (dd, J = 5.1, 3.5 Hz, 1H), 6.67−6.56 (m, 1H), 6.42 (s, 1H), 6.33−6.24 (m, 1H), 4.67 (d, J = 14.6 Hz, 1H), 4.42 (d, J = 14.7 Hz, 1H), 3.67−3.54 (m, 2H), 3.38 (d, J = 11.7 Hz, 1H), 3.01−2.88 (m, 2H), 2.72 (t, J = 11.0 Hz, 1H), 2.54 (td, J = 6.6, 5.9, 3.4 Hz, 1H), 1.90 (s, 1H), 1.81−1.75 (m, 1H), 1.67 (td, J = 11.6, 5.7 Hz, 2H), 1.47 (s, 6H), 1.35−1.32 (m, 2H), 1.08−1.02 (m, 2H), 0.85−0.73 (m, 4H). ^{13}C NMR (126 MHz, Chloroform-d): δ 176.8, 173.8, 154.3, 152.7, 144.1, 137.6, 133.3, 129.7, 128.3, 128.0, 126.1, 124.7, 123.0, 112.2, 111.3, 109.6, 81.4, 51.9, 50.0, 49.5, 39.8, 31.1, 29.8, 27.8, 24.6, 24.5, 9.6, 9.0, 6.2. HRMS (ESI): calcd for $C_{33}H_{39}N_3O_5S_2$ (M − H)$^-$, 620.2258; found, 620.2262. HPLC purity 96.9%, t_R = 14.26 min.

***N*-Cyclopropyl-1-(3-((2-methyl-1-((1-methylethyl)-sulfonamido)-1-oxopropan-2-yl)oxy)phenyl)-*N*-(4-(thiophen-2-yl)benzyl)piperidine-3-carboxamide (20).** ^{1}H NMR (500 MHz,

https://doi.org/10.1021/acs.jmedchem.1c00046
J. Med. Chem. 2021, 64, 5886−5904

Chloroform-*d*): δ 8.72 (s, 1H), 7.54−7.45 (m, 2H), 7.23−7.16 (m, 4H), 7.07 (t, *J* = 8.2 Hz, 1H), 7.00 (dd, *J* = 5.1, 3.6 Hz, 1H), 6.67−6.56 (m, 1H), 6.42 (s, 1H), 6.29 (dd, *J* = 8.2, 2.2 Hz, 1H), 4.67 (d, *J* = 14.7 Hz, 1H), 4.43 (d, *J* = 14.7 Hz, 1H), 3.77 (hept, *J* = 6.9 Hz, 1H), 3.66−3.56 (m, 2H), 3.37 (t, *J* = 10.7 Hz, 1H), 2.97 (t, *J* = 11.7 Hz, 1H), 2.76−2.68 (m, 1H), 2.59−2.51 (m, 1H), 1.91 (d, *J* = 10.0 Hz, 1H), 1.82−1.74 (m, 1H), 1.68 (td, *J* = 10.2, 8.8, 3.1 Hz, 2H), 1.47 (s, 6H), 1.35 (dd, *J* = 6.9, 1.4 Hz, 6H), 0.86−0.73 (m, 4H). ^{13}C NMR (126 MHz, Chloroform-*d*): δ 176.8, 174.1, 154.2, 152.7, 144.1, 137.6, 133.3, 129.7, 128.3, 128.0, 126.1, 124.7, 123.0, 112.3, 111.6, 109.8, 81.6, 54.1, 51.9, 49.9, 49.5, 39.8, 29.8, 27.8, 24.6, 24.5, 16.0, 15.9, 9.6, 9.0. HRMS (ESI): calcd for $C_{33}H_{41}N_3O_5S_2$ $(M-H)^-$, 622.2415; found, 622.2419. HPLC purity 96.9%, t_R = 14.33 min.

***N*-Cyclopropyl-1-(3-((2-methyl-1-oxo-1-(phenylsulfonamido)propan-2-yl)oxy)phenyl)-*N*-(4-(thiophen-2-yl)benzyl)piperidine-3-carboxamide (21).** ^{1}H NMR (500 MHz, Chloroform-*d*): δ 9.04 (s, 1H), 8.02−7.94 (m, 2H), 7.64−7.57 (m, 1H), 7.48 (dt, *J* = 7.8, 3.8 Hz, 4H), 7.22−7.16 (m, 4H), 7.03−6.99 (m, 1H), 6.91 (t, *J* = 8.2 Hz, 1H), 6.62−6.51 (m, 1H), 6.35 (t, *J* = 2.5 Hz, 1H), 5.99 (dd, *J* = 8.0, 2.3 Hz, 1H), 4.67 (d, *J* = 14.6 Hz, 1H), 4.43 (d, *J* = 14.7 Hz, 1H), 3.64−3.52 (m, 2H), 3.36 (t, *J* = 10.9 Hz, 1H), 2.94 (t, *J* = 11.7 Hz, 1H), 2.67 (t, *J* = 11.1 Hz, 1H), 2.55 (tt, *J* = 7.2, 4.1 Hz, 1H), 1.90 (d, *J* = 10.8 Hz, 1H), 1.77−1.63 (m, 3H), 1.36 (s, 6H), 0.84−0.74 (m, 4H). ^{13}C NMR (126 MHz, Chloroform-*d*): δ 176.8, 172.9, 154.3, 152.7, 144.1, 138.2, 137.6, 134.1, 133.3, 129.6, 129.0, 128.5, 128.3, 128.0, 126.1, 124.7, 123.0, 112.0, 110.6, 109.3, 81.2, 51.9, 49.8, 49.6, 39.8, 29.8, 27.8, 24.5, 24.4, 9.6, 9.0. HRMS (ESI): calcd for $C_{36}H_{39}N_3O_5S_2$ $(M-H)^-$, 656.2258; found, 656.2252. HPLC purity 96.2%, t_R = 14.70 min.

***N*-Cyclopropyl-1-(3-((1-((3-methoxyphenyl)sulfonamido)-2-methyl-1-oxopropan-2-yl)oxy)phenyl)-*N*-(4-(thiophen-2-yl)benzyl)piperidine-3-carboxamide (22).** ^{1}H NMR (500 MHz, Chloroform-*d*): δ 9.05 (s, 1H), 7.55 (dt, *J* = 7.8, 1.2 Hz, 1H), 7.50−7.46 (m, 3H), 7.39−7.35 (m, 1H), 7.22−7.15 (m, 4H), 7.11 (ddd, *J* = 8.3, 2.7, 0.9 Hz, 1H), 6.99 (dd, *J* = 5.1, 3.6 Hz, 1H), 6.91 (t, *J* = 8.2 Hz, 1H), 6.56 (dd, *J* = 8.3, 2.3 Hz, 1H), 6.39−6.28 (m, 1H), 5.99 (dd, *J* = 8.1, 2.2 Hz, 1H), 4.66 (d, *J* = 14.7 Hz, 1H), 4.43 (d, *J* = 14.6 Hz, 1H), 3.77 (s, 3H), 3.62−3.52 (m, 2H), 3.35 (dq, *J* = 11.4, 5.8, 4.3 Hz, 1H), 2.94 (t, *J* = 11.6 Hz, 1H), 2.70−2.63 (m, 1H), 2.54 (tt, *J* = 6.9, 4.1 Hz, 1H), 1.89 (d, *J* = 10.9 Hz, 1H), 1.76−1.63 (m, 3H), 1.36 (s, 6H), 0.85−0.73 (m, 4H). ^{13}C NMR (126 MHz, Chloroform-*d*): δ 176.8, 172.9, 159.7, 154.3, 152.7, 144.1, 139.3, 137.6, 133.3, 130.0, 129.6, 128.3, 128.0, 126.1, 124.7, 123.0, 120.9, 120.5, 112.6, 111.9, 110.6, 109.2, 81.2, 55.7, 51.9, 49.8, 49.6, 39.8, 29.8, 27.8, 24.5, 24.4, 9.6, 9.0. HRMS (ESI): calcd for $C_{37}H_{41}N_3O_6S_2$ $(M-H)^-$, 686.2364; found, 686.2360. HPLC purity 99.6%, t_R = 14.75 min.

***N*-Cyclopropyl-1-(3-((1-((4-methoxyphenyl)sulfonamido)-2-methyl-1-oxopropan-2-yl)oxy)phenyl)-*N*-(4-(thiophen-2-yl)benzyl)piperidine-3-carboxamide (23).** ^{1}H NMR (500 MHz, Chloroform-*d*): δ 9.07 (s, 1H), 8.02−7.95 (m, 2H), 7.56 (d, *J* = 8.0 Hz, 2H), 7.31−7.23 (m, 4H), 7.07 (dd, *J* = 5.1, 3.6 Hz, 1H), 7.02−6.97 (m, 3H), 6.64 (dd, *J* = 8.6, 2.2 Hz, 1H), 6.41 (t, *J* = 2.4 Hz, 1H), 6.08 (dd, *J* = 8.1, 2.2 Hz, 1H), 4.74 (d, *J* = 14.7 Hz, 1H), 4.51 (d, *J* = 14.7 Hz, 1H), 3.89 (s, 3H), 3.65 (t, *J* = 12.7 Hz, 2H), 3.42 (d, *J* = 10.8 Hz, 1H), 3.01 (t, *J* = 11.7 Hz, 1H), 2.75 (t, *J* = 11.1 Hz, 1H), 2.62 (tt, *J* = 7.1, 4.0 Hz, 1H), 1.97 (d, *J* = 10.8 Hz, 1H), 1.83 (d, *J* = 11.1 Hz, 1H), 1.68 (d, *J* = 35.2 Hz, 2H), 1.43 (s, 6H), 0.91−0.82 (m, 4H). ^{13}C NMR (126 MHz, Chloroform-*d*): δ 176.8, 172.9, 164.0, 154.4, 152.7, 144.1, 137.7, 133.3, 130.9, 129.6, 129.5, 128.6, 128.3, 128.0, 126.1, 124.7, 123.0, 114.1, 111.9, 110.7, 109.2, 81.2, 55.7, 51.9, 49.8, 39.8, 29.8, 27.8, 24.5, 24.4, 9.6, 9.0. HRMS (ESI): calcd for $C_{37}H_{41}N_3O_6S_2$ $(M-H)^-$, 686.2364; found, 686.2367. HPLC purity 96.5%, t_R = 14.69 min.

***N*-Cyclopropyl-1-(3-((1-((3-hydroxyphenyl)sulfonamido)-2-methyl-1-oxopropan-2-yl)oxy)phenyl)-*N*-(4-(thiophen-2-yl)benzyl)piperidine-3-carboxamide (24).** ^{1}H NMR (500 MHz, Chloroform-*d*): δ 7.53−7.48 (m, 3H), 7.37 (t, *J* = 2.1 Hz, 1H), 7.29 (t, *J* = 8.0 Hz, 1H), 7.22−7.15 (m, 4H), 7.07−7.04 (m, 1H), 7.00−6.95 (m, 2H), 6.64−6.53 (m, 1H), 6.23 (s, 1H), 6.14 (dd, *J* = 8.0, 2.2 Hz, 1H), 4.72 (d, *J* = 14.7 Hz, 1H), 4.42 (d, *J* = 14.7 Hz, 1H), 3.53−3.38 (m, 3H), 2.86 (t, *J* = 11.5 Hz, 1H), 2.59−2.50 (m, 2H), 1.90 (d, *J* = 8.1 Hz, 1H), 1.75 (dt, *J* = 9.2, 2.9 Hz, 1H), 1.67−1.60 (m, 2H), 1.41 (s, 3H), 1.32 (s, 3H), 0.87−0.77 (m, 4H). ^{13}C NMR (126 MHz, Chloroform-*d*): δ 177.6, 173.0, 157.1, 154.6, 152.7, 144.0, 139.0, 137.1, 133.5, 130.1, 129.8, 128.2, 128.0, 126.2, 124.8, 123.1, 122.2, 120.3, 114.6, 113.1, 112.0, 108.5, 81.3, 52.0, 50.3, 39.9, 30.1, 27.6, 25.4, 24.5, 23.9, 9.7, 8.9. HRMS (ESI): calcd for $C_{36}H_{39}N_3O_6S_2$ $(M-H)^-$, 672.2208; found, 672.2201. HPLC purity 99.4%, t_R = 14.07 min.

1-(3-((1-((3-Cyanophenyl)sulfonamido)-2-methyl-1-oxopropan-2-yl)oxy)phenyl)-*N*-cyclopropyl-*N*-(4-(thiophen-2-yl)-benzyl)piperidine-3-carboxamide (25). ^{1}H NMR (500 MHz, Chloroform-*d*): δ 8.30 (dq, *J* = 4.6, 1.4 Hz, 2H), 7.93 (dt, *J* = 7.8, 1.4 Hz, 1H), 7.70 (t, *J* = 8.2 Hz, 1H), 7.58−7.52 (m, 2H), 7.29 (dd, *J* = 3.6, 1.2 Hz, 1H), 7.27−7.23 (m, 3H), 7.07 (dd, *J* = 5.1, 3.6 Hz, 1H), 7.01 (t, *J* = 8.2 Hz, 1H), 6.74−6.62 (m, 1H), 6.42 (s, 1H), 6.12−5.97 (m, 1H), 4.74 (d, *J* = 14.6 Hz, 1H), 4.51 (d, *J* = 14.7 Hz, 1H), 3.70−3.62 (m, 2H), 3.43 (s, 1H), 3.02 (t, *J* = 11.7 Hz, 1H), 2.80−2.71 (m, 1H), 2.62 (tt, *J* = 6.9, 4.1 Hz, 1H), 2.01−1.95 (m, 1H), 1.86−1.81 (m, 1H), 1.74 (td, *J* = 10.7, 9.1, 3.2 Hz, 2H), 1.45 (s, 6H), 0.93−0.82 (m, 4H). ^{13}C NMR (126 MHz, Chloroform-*d*): δ 176.7, 173.1, 154.1, 152.8, 144.0, 139.8, 137.6, 137.1, 133.3, 132.7, 132.1, 130.0, 129.7, 128.3, 128.0, 126.1, 124.7, 123.0, 116.9, 113.7, 112.2, 110.3, 109.1, 81.2, 51.8, 49.8, 49.6, 39.8, 29.8, 27.8, 24.5, 24.43, 24.38, 9.6, 9.0. HRMS (ESI): calcd for $C_{37}H_{38}N_4O_5S_2$ $(M-H)^-$, 681.2211; found, 681.2219. HPLC purity 98.2%, t_R = 14.54 min.

1-(3-((1-((4-Cyanophenyl)sulfonamido)-2-methyl-1-oxopropan-2-yl)oxy)phenyl)-*N*-cyclopropyl-*N*-(4-(thiophen-2-yl)-benzyl)piperidine-3-carboxamide (26). ^{1}H NMR (500 MHz, Chloroform-*d*): δ 8.18−8.14 (m, 2H), 7.85−7.82 (m, 2H), 7.58−7.53 (m, 2H), 7.30−7.23 (m, 4H), 7.07 (dd, *J* = 5.1, 3.5 Hz, 1H), 7.01 (t, *J* = 8.2 Hz, 1H), 6.67 (d, *J* = 8.4 Hz, 1H), 6.42 (s, 1H), 6.08 (d, *J* = 8.0 Hz, 1H), 4.74 (d, *J* = 14.7 Hz, 1H), 4.51 (d, *J* = 14.7 Hz, 1H), 3.65 (d, *J* = 11.7 Hz, 2H), 3.40 (d, *J* = 34.3 Hz, 1H), 3.02 (t, *J* = 11.7 Hz, 1H), 2.75 (t, *J* = 11.5 Hz, 1H), 2.62 (tt, *J* = 6.9, 4.1 Hz, 1H), 1.98 (d, *J* = 9.5 Hz, 1H), 1.88−1.83 (m, 1H), 1.74 (dd, *J* = 14.5, 5.8 Hz, 2H), 1.44 (s, 6H), 0.94−0.82 (m, 4H). ^{13}C NMR (126 MHz, Chloroform-*d*): δ 176.7, 173.1, 154.1, 152.8, 144.0, 142.2, 137.6, 133.3, 132.7, 129.7, 129.2, 128.3, 128.0, 126.1, 124.8, 123.0, 117.7, 117.1, 112.3, 110.7, 109.3, 81.3, 51.9, 49.9, 49.6, 39.8, 29.8, 27.7, 24.5, 24.4, 24.3, 9.7, 8.9. HRMS (ESI): calcd for $C_{37}H_{38}N_4O_5S_2$ $(M-H)^-$, 681.2211; found, 681.2212. HPLC purity 98.7%, t_R = 14.62 min.

***(R)*-*N*-Cyclopropyl-1-(3-((1-((3-methoxyphenyl)-sulfonamido)-2-methyl-1-oxopropan-2-yl)oxy)phenyl)-*N*-(4-(thiophen-2-yl)benzyl)piperidine-3-carboxamide (27).** $[\alpha]_D^{25}$ −16.10° (*c* 0.955, MeOH). ^{1}H NMR (500 MHz, Chloroform-*d*): δ 9.08 (s, 1H), 7.63 (dt, *J* = 7.8, 1.2 Hz, 1H), 7.58−7.53 (m, 3H), 7.45 (t, *J* = 8.0 Hz, 1H), 7.29−7.23 (m, 4H), 7.19 (ddd, *J* = 8.3, 2.6, 0.9 Hz, 1H), 7.07 (dd, *J* = 5.1, 3.6 Hz, 1H), 6.99 (t, *J* = 8.2 Hz, 1H), 6.64 (d, *J* = 8.3 Hz, 1H), 6.42 (s, 1H), 6.12−6.01 (m, 1H), 4.74 (d, *J* = 14.7 Hz, 1H), 4.50 (d, *J* = 14.7 Hz, 1H), 3.85 (s, 3H), 3.69−3.60 (m, 2H), 3.43 (s, 1H), 3.02 (t, *J* = 11.6 Hz, 1H), 2.75 (t, *J* = 11.7 Hz, 1H), 2.62 (tt, *J* = 6.8, 4.0 Hz, 1H), 1.97 (d, *J* = 10.8 Hz, 1H), 1.83 (d, *J* = 11.0 Hz, 1H), 1.75−1.72 (m, 1H), 1.64 (s, 1H), 1.44 (s, 6H), 0.93−0.81 (m, 4H). ^{13}C NMR (126 MHz, Chloroform-*d*): δ 176.8, 172.8, 159.7, 154.3, 152.7, 144.1, 139.2, 137.6, 133.3, 130.2, 130.0, 129.6, 128.3, 128.0, 126.1, 124.7, 123.0, 120.9, 120.6, 119.2, 118.5, 112.6, 111.9, 111.1, 110.6, 109.2, 81.2, 55.73, 55.68, 51.9, 49.8, 49.6, 39.8, 29.8, 27.8, 24.4, 24.4, 9.6, 9.0. HRMS (ESI): calcd for $C_{37}H_{41}N_3O_6S_2$ $(M-H)^-$, 686.2364; found, 686.2348. HPLC purity 96.3%, t_R = 14.70 min.

***(S)*-*N*-Cyclopropyl-1-(3-((1-((3-methoxyphenyl)-sulfonamido)-2-methyl-1-oxopropan-2-yl)oxy)phenyl)-*N*-(4-(thiophen-2-yl)benzyl)piperidine-3-carboxamide (28).** $[\alpha]_D^{25}$ +14.38° (*c* 0.955, MeOH). ^{1}H NMR (500 MHz, Chloroform-*d*): δ 9.06 (s, 1H), 7.63 (ddd, *J* = 7.8, 1.8, 1.0 Hz, 1H), 7.59−7.49 (m, 3H), 7.47−7.43 (m, 1H), 7.29 (dd, *J* = 3.6, 1.2 Hz, 1H), 7.27 (d, *J* = 6.1 Hz, 1H), 7.24 (d, *J* = 8.0 Hz, 2H), 7.19 (ddd, *J* = 8.3, 2.6, 0.9 Hz, 1H), 7.07 (dd, *J* = 5.1, 3.6 Hz, 1H), 6.99 (t, *J* = 8.2 Hz, 1H), 6.64 (dd, *J* = 8.1, 2.4 Hz, 1H), 6.42 (t, *J* = 2.4 Hz, 1H), 6.05 (dd, *J* = 7.8, 2.3 Hz, 1H), 4.74 (d, *J* = 14.7 Hz, 1H), 4.50 (d, *J* = 14.6 Hz, 1H), 3.85 (d, *J* = 1.4 Hz, 3H), 3.69−3.60 (m, 2H), 3.43 (tt, *J* = 11.0, 3.7 Hz, 1H), 3.01 (dd, *J* = 12.4, 11.0 Hz, 1H), 2.75 (td, *J* = 12.2, 2.9 Hz, 1H), 2.66−2.58 (m, 1H), 1.97 (d, *J* = 11.0 Hz, 1H), 1.83 (dq, *J* = 11.8, 3.2, 2.7 Hz, 1H), 1.73 (d, *J* = 9.2 Hz, 1H), 1.62 (d, *J* = 6.9 Hz, 1H), 1.44 (s, 6H), 0.93−0.81 (m, 4H). ^{13}C

https://doi.org/10.1021/acs.jmedchem.1c00046
J. Med. Chem. 2021, 64, 5886−5904

NMR (126 MHz, $CDCl_3$): δ 176.8, 172.8, 159.7, 154.3, 152.7, 144.1, 139.2, 137.6, 133.3, 130.0, 129.6, 128.3, 128.1, 126.1, 124.8, 123.0, 121.0, 120.6, 112.6, 111.9, 110.6, 109.2, 81.2, 55.7, 51.9, 49.8, 49.5, 39.8, 29.8, 27.8, 24.5, 24.4, 9.6, 9.0. HRMS (ESI): calcd for $C_{37}H_{41}N_3O_6S_2$ $(M - H)^-$, 686.2364; found, 686.2345. HPLC purity 97.3%, t_R = 14.69 min.

(*R*)-1-(3-((1-((4-Cyanophenyl)sulfonamido)-2-methyl-1-oxopropan-2-yl)oxy)phenyl)-*N*-cyclopropyl-*N*-(4-(thiophen-2-yl)benzyl)piperidine-3-carboxamide (29). $[\alpha]_D^{25}$ −13.90° (c 1.104, MeOH). ^{1}H NMR (500 MHz, Chloroform-*d*): δ 8.20−8.12 (m, 2H), 7.88−7.81 (m, 2H), 7.62−7.52 (m, 2H), 7.29 (dd, *J* = 3.6, 1.2 Hz, 1H), 7.28−7.26 (m, 1H), 7.24 (d, *J* = 8.1 Hz, 2H), 7.11−6.95 (m, 2H), 6.67 (d, *J* = 8.3 Hz, 1H), 6.42 (s, 1H), 6.08 (d, *J* = 8.0 Hz, 1H), 4.74 (d, *J* = 14.7 Hz, 1H), 4.51 (d, *J* = 14.7 Hz, 1H), 3.65 (d, *J* = 12.1 Hz, 2H), 3.43 (s, 1H), 3.02 (t, *J* = 11.6 Hz, 1H), 2.76 (t, *J* = 11.9 Hz, 1H), 2.62 (tt, *J* = 6.7, 4.1 Hz, 1H), 1.98 (d, *J* = 9.7 Hz, 1H), 1.85 (d, *J* = 9.7 Hz, 1H), 1.73 (d, *J* = 8.7 Hz, 1H), 1.57 (d, *J* = 7.9 Hz, 1H), 1.44 (s, 6H), 0.95−0.82 (m, 4H). ^{13}C NMR (126 MHz, Chloroform-*d*): δ 176.7, 173.0, 154.1, 144.0, 142.1, 137.6, 133.4, 132.7, 129.7, 129.2, 128.3, 128.0, 126.1, 124.8, 123.0, 117.7, 117.1, 112.3, 110.7, 109.3, 81.3, 51.9, 49.9, 49.6, 39.8, 29.8, 27.7, 24.5, 24.4, 24.3, 9.7, 8.9. HRMS (ESI): calcd for $C_{37}H_{38}N_4O_5S_2$ $(M - H)^-$, 681.2211; found, 681.2217. HPLC purity 96.0%, t_R = 14.62 min.

(*S*)-((4-Cyanophenyl)sulfonyl)(2-(3-(3-(cyclopropyl(4-(thiophen-2-yl)benzyl)carbamoyl)piperidin-1-yl)phenoxy)-2-methylpropanoyl)amide (30). $[\alpha]_D^{25}$ +16.92° (*c* 0.881, MeOH). ^{1}H NMR (500 MHz, Chloroform-*d*): δ 8.20−8.12 (m, 2H), 7.88−7.80 (m, 2H), 7.60−7.50 (m, 2H), 7.29 (dd, *J* = 3.5, 1.2 Hz, 1H), 7.28−7.26 (m, 1H), 7.24 (d, *J* = 7.9 Hz, 2H), 7.12−6.97 (m, 2H), 6.67 (d, *J* = 8.3 Hz, 1H), 6.42 (s, 1H), 6.08 (d, *J* = 8.0 Hz, 1H), 4.74 (d, *J* = 14.7 Hz, 1H), 4.51 (d, *J* = 14.7 Hz, 1H), 3.65 (dd, *J* = 11.8, 3.6 Hz, 2H), 3.45 (d, *J* = 12.3 Hz, 1H), 3.02 (t, *J* = 11.6 Hz, 1H), 2.76 (t, *J* = 11.6 Hz, 1H), 2.62 (tt, *J* = 6.9, 4.1 Hz, 1H), 1.98 (d, *J* = 9.9 Hz, 1H), 1.89−1.81 (m, 1H), 1.75 (d, *J* = 8.9 Hz, 1H), 1.62 (s, 1H), 1.44 (s, 6H), 0.93−0.81 (m, 4H). ^{13}C NMR (126 MHz, Chloroform-*d*): δ 176.7, 173.0, 154.1, 152.8, 144.0, 142.1, 137.6, 133.4, 132.7, 129.7, 129.2, 128.3, 128.0, 126.1, 124.8, 123.0, 117.7, 117.1, 112.3, 110.7, 109.3, 81.3, 51.9, 49.9, 39.8, 29.8, 27.7, 24.5, 24.4, 24.3, 9.7, 8.9. HRMS (ESI): calcd for $C_{37}H_{38}N_4O_5S_2$ $(M - H)^-$, 681.2211; found, 681.2199. HPLC purity 97.0%, t_R = 14.61 min.

***tert*-Butyl 2-(3-bromophenoxy)-2-methylpropanoate (31).** ^{1}H NMR (500 MHz, Chloroform-*d*): δ 7.16−7.04 (m, 2H), 7.01 (dd, *J* = 2.7, 1.3 Hz, 1H), 6.82−6.71 (m, 1H), 1.56 (s, 6H), 1.44 (s, 9H). ^{13}C NMR (126 MHz, Chloroform-*d*): δ 172.8, 156.5, 130.1, 124.6, 122.2, 121.8, 117.3, 82.0, 79.8, 27.8, 25.3. MS (ESI) *m*/*z*: 315.1 $[M + H]^+$.

***N*-(4-Isopropylbenzyl)ethanamine (32a).** ^{1}H NMR (500 MHz, Chloroform-*d*): δ 7.24 (d, *J* = 8.2 Hz, 2H), 7.21−7.16 (m, 2H), 3.76 (s, 2H), 2.89 (hept, *J* = 6.9 Hz, 1H), 2.69 (q, *J* = 7.1 Hz, 2H), 1.25 (d, *J* = 6.9 Hz, 6H), 1.13 (t, *J* = 7.1 Hz, 3H). ^{13}C NMR (126 MHz, Chloroform-*d*): δ 147.5, 137.9, 128.1, 126.4, 53.8, 43.7, 33.8, 24.1, 15.3. MS (ESI) *m*/*z*: 178.2 $[M + H]^+$

***N*-(4-Isopropylbenzyl)propan-2-amine (32b).** ^{1}H NMR (500 MHz, Chloroform-*d*): δ 7.26−7.21 (m, 2H), 7.20−7.16 (m, 2H), 3.75 (s, 2H), 3.00−2.65 (m, 2H), 1.24 (d, *J* = 6.9 Hz, 6H), 1.10 (d, *J* = 6.2 Hz, 6H). ^{13}C NMR (126 MHz, Chloroform-*d*): δ 147.4, 138.2, 128.1, 126.4, 51.4, 48.1, 33.8, 24.0, 23.0. MS (ESI) *m*/*z*: 192.3 $[M + H]^+$.

***N*-(4-Isopropylbenzyl)cyclopropanamine (32c).** ^{1}H NMR (500 MHz, Chloroform-*d*): δ 7.25−7.22 (m, 2H), 7.20−7.17 (m, 2H), 3.81 (s, 2H), 2.90 (hept, *J* = 6.9 Hz, 1H), 2.22−2.12 (m, 1H), 1.25 (d, *J* = 6.9 Hz, 6H), 0.48−0.35 (m, 4H). ^{13}C NMR (126 MHz, Chloroform-*d*): δ 147.5, 138.0, 128.2, 126.4, 53.5, 33.8, 30.1, 24.1, 6.5. MS (ESI) *m*/*z*: 190.2 $[M + H]^+$.

***tert*-Butyl 3-((4-isopropylbenzyl)carbamoyl)piperidine-1-carboxylate (33a).** ^{1}H NMR (500 MHz, Chloroform-*d*): δ 7.15 (s, 4H), 4.37 (d, *J* = 19.2 Hz, 2H), 4.03−3.60 (m, 2H), 3.14 (dd, *J* = 13.5, 9.3 Hz, 1H), 2.86 (hept, *J* = 6.8 Hz, 2H), 2.28 (dq, *J* = 9.8, 5.3, 4.9 Hz, 1H), 1.91−1.77 (m, 2H), 1.69−1.54 (m, 1H), 1.38 (s, 10H), 1.21 (d, *J* = 7.0 Hz, 6H). ^{13}C NMR (126 MHz, Chloroform-*d*): δ 172.9, 154.8, 148.1, 135.6, 127.8, 126.7, 79.8, 45.9, 44.6, 43.2, 43.0, 33.8, 28.4, 27.8, 24.2, 24.0. MS (ESI) *m*/*z*: 361.3 $[M + H]^+$, 383.3 $[M + Na]^+$.

***tert*-Butyl 3-((4-isopropylphenethyl)carbamoyl)piperidine-1-carboxylate (33b).** ^{1}H NMR (500 MHz, Chloroform-*d*): δ 7.12 (dd, *J* = 8.2, 1.8 Hz, 2H), 7.03 (dd, *J* = 8.0, 1.6 Hz, 2H), 6.59−5.89 (m, 1H), 4.09−3.50 (m, 2H), 3.42 (qt, *J* = 13.3, 7.0 Hz, 2H), 3.04 (s, 1H), 2.87−2.82 (m, 1H), 2.74−2.71 (m, 4H), 2.16 (dt, *J* = 12.5, 6.2 Hz, 1H), 1.78 (d, *J* = 8.5 Hz, 1H), 1.56 (t, *J* = 12.7 Hz, 1H), 1.39 (d, *J* = 1.6 Hz, 10H), 1.20 (dd, *J* = 7.0, 1.5 Hz, 6H). MS (ESI) *m*/*z*: 375.3 $[M + H]^+$, 397.3 $[M + Na]^+$.

***tert*-Butyl 3-((4-isopropylbenzyl)(methyl)carbamoyl)piperidine-1-carboxylate (33c).** ^{1}H NMR (500 MHz, Chloroform-*d*): δ 7.24−7.12 (m, 2H), 7.11−6.89 (m, 2H), 4.51 (s, 2H), 4.16 (s, 1H), 4.06 (s, 1H), 2.95 (s, 2H), 2.90−2.79 (m, 3H), 2.70−2.45 (m, 2H), 2.02−1.54 (m, 3H), 1.53−1.30 (m, 10H), 1.21 (t, *J* = 6.9 Hz, 6H). ^{13}C NMR (126 MHz, Chloroform-*d*): δ 173.8, 173.1, 154.7, 154.5, 148.4, 148.0, 134.5, 133.9, 127.9, 127.0, 126.6, 126.2, 79.6, 79.5, 52.8, 50.4, 46.5, 44.3, 39.5, 34.6, 33.83, 33.76, 28.44, 28.39, 28.1, 27.6, 24.7, 24.6, 23.97, 23.95. MS (ESI) *m*/*z*: 375.3 $[M + H]^+$.

***tert*-Butyl 3-(ethyl(4-isopropylbenzyl)carbamoyl)piperidine-1-carboxylate (33d).** ^{1}H NMR (500 MHz, Chloroform-*d*): δ 7.20−7.14 (m, 1H), 7.14−6.90 (m, 3H), 4.85−3.96 (m, 4H), 3.26 (s, 2H), 2.84 (dp, *J* = 13.7, 6.9 Hz, 2H), 2.60 (tt, *J* = 31.9, 17.1 Hz, 2H), 1.97−1.55 (m, 3H), 1.38 (d, *J* = 30.3 Hz, 10H), 1.19 (dd, *J* = 8.0, 6.9 Hz, 6H), 1.08 (dt, *J* = 48.7, 7.1 Hz, 3H). ^{13}C NMR (126 MHz, Chloroform-*d*): δ 173.3, 173.1, 154.6, 154.5, 148.2, 147.8, 135.0, 134.4, 127.8, 126.9, 126.56, 126.2, 79.5, 79.4, 53.4, 50.0, 47.3, 44.6, 43.9, 41.3, 40.6, 39.5, 33.7 (d, *J* = 2.8 Hz), 28.43, 28.37, 28.1, 24.6, 24.0, 23.9, 14.3, 12.6. MS (ESI) *m*/*z*: 389.3 $[M + H]^+$.

***tert*-Butyl 3-(isopropyl(4-isopropylbenzyl)carbamoyl)piperidine-1-carboxylate (33e).** ^{1}H NMR (500 MHz, Chloroform-*d*): δ 7.19−7.12 (m, 1H), 7.12−6.97 (m, 3H), 4.94−3.85 (m, 5H), 3.19−2.20 (m, 4H), 2.04−1.62 (m, 2H), 1.64−1.52 (m, 1H), 1.44 (s, 4H), 1.36 (s, 6H), 1.29−1.10 (m, 9H), 1.04 (d, *J* = 6.8 Hz, 3H). ^{13}C NMR (126 MHz, Chloroform-*d*): δ 174.0, 173.3, 154.6, 154.5, 147.8, 147.0, 136.7, 136.0, 126.7, 126.6, 126.3, 125.6, 79.5, 79.4, 53.4, 48.5, 47.1, 46.5, 45.5, 44.6, 43.6, 40.7, 39.7, 33.7, 28.5, 28.4, 28.2, 24.8, 24.4, 24.0, 23.9, 22.0, 21.9, 20.2. MS (ESI) *m*/*z*: 403.3 $[M + H]^+$, 425.3 $[M + Na]^+$.

***tert*-Butyl 3-(cyclopropyl(4-isopropylbenzyl)carbamoyl)piperidine-1-carboxylate (33f).** ^{1}H NMR (500 MHz, Chloroform-*d*): δ 7.12 (t, *J* = 6.7 Hz, 4H), 4.91−3.94 (m, 4H), 3.19 (tt, *J* = 11.5, 3.8 Hz, 1H), 2.87 (dq, *J* = 13.8, 6.8 Hz, 2H), 2.65 (d, *J* = 69.8 Hz, 2H), 1.90 (d, *J* = 13.3 Hz, 1H), 1.85−1.63 (m, 2H), 1.45 (s, 10H), 1.22 (d, *J* = 6.9 Hz, 6H), 0.97−0.70 (m, 4H). ^{13}C NMR (126 MHz, Chloroform-*d*): δ 176.2, 154.7, 147.7, 135.5, 127.6, 126.5, 79.5, 49.4, 47.3, 44.8, 40.3, 33.7, 29.6, 28.5, 27.8, 24.7, 24.0, 9.3. MS (ESI) *m*/*z*: 401.4 $[M + H]^+$, 423.3 $[M + Na]^+$.

***tert*-Butyl 2-(3-(3-((4-isopropylbenzyl)carbamoyl)piperidin-1-yl)phenoxy)-2-methylpropanoate (34a).** ^{1}H NMR (500 MHz, Chloroform-*d*): δ 7.18 (d, *J* = 1.6 Hz, 4H), 7.06 (t, *J* = 8.2 Hz, 1H), 6.90 (t, *J* = 5.7 Hz, 1H), 6.54 (dd, *J* = 8.3, 2.3 Hz, 1H), 6.49 (t, *J* = 2.3 Hz, 1H), 6.34 (dd, *J* = 8.2, 2.3 Hz, 1H), 4.42 (d, *J* = 5.6 Hz, 2H), 3.39 (dd, *J* = 12.5, 3.6 Hz, 1H), 3.31−3.15 (m, 2H), 3.02 (ddd, *J* = 11.8, 8.4, 3.1 Hz, 1H), 2.88 (p, *J* = 6.9 Hz, 1H), 2.55 (tt, *J* = 8.0, 4.1 Hz, 1H), 2.02−1.72 (m, 3H), 1.66 (tq, *J* = 8.7, 4.4 Hz, 1H), 1.55 (s, 6H), 1.42 (d, *J* = 0.9 Hz, 9H), 1.23 (d, *J* = 6.9 Hz, 6H). ^{13}C NMR (126 MHz, Chloroform-*d*): δ 174.1, 173.5, 156.7, 152.5, 148.0, 135.8, 129.2, 127.7, 126.7, 111.1, 110.1, 108.2, 81.6, 79.3, 52.7, 50.6, 43.1, 42.4, 33.8, 27.8, 27.4, 25.5, 25.4, 24.0, 23.5. MS (ESI) *m*/*z*: 495.4 $[M + H]^+$.

***tert*-Butyl 2-(3-(3-((4-isopropylphenethyl)carbamoyl)-piperidin-1-yl)phenoxy)-2-methylpropanoate (34b).** ^{1}H NMR (500 MHz, Chloroform-*d*): δ 7.18−7.01 (m, 5H), 6.71−6.60 (m, 1H), 6.54−6.45 (m, 2H), 6.36 (dd, *J* = 8.1, 2.2 Hz, 1H), 3.63−3.42 (m, 2H), 3.28−3.13 (m, 2H), 3.10 (ddd, *J* = 11.4, 6.7, 4.2 Hz, 1H), 3.00 (ddd, *J* = 11.8, 7.2, 4.1 Hz, 1H), 2.91−2.81 (m, *J* = 6.7 Hz, 1H), 2.79 (td, *J* = 6.9, 5.1 Hz, 2H), 2.47 (td, *J* = 6.6, 3.3 Hz, 1H), 1.84 (dtd, *J* = 12.1, 7.5, 4.4 Hz, 1H), 1.78−1.67 (m, 1H), 1.65−1.51 (m, 8H), 1.44 (s, 9H), 1.22 (d, *J* = 7.0 Hz, 6H). MS (ESI) *m*/*z*: 509.4 $[M + H]^+$.

***tert*-Butyl 2-(3-(3-((4-isopropylbenzyl)(methyl)carbamoyl)-piperidin-1-yl)phenoxy)-2-methylpropanoate (34c).** ^{1}H NMR

https://doi.org/10.1021/acs.jmedchem.1c00046
J. Med. Chem. 2021, 64, 5886−5904

(500 MHz, Chloroform-*d*): δ 7.17−7.06 (m, 3H), 7.04−6.83 (m, 2H), 6.57−6.30 (m, 2H), 6.21 (ddd, *J* = 16.6, 8.1, 2.2 Hz, 1H), 4.62−4.28 (m, 2H), 3.87−3.51 (m, 2H), 3.00−2.76 (m, 6H), 2.67 (dtd, *J* = 18.5, 12.0, 2.7 Hz, 1H), 2.05−1.61 (m, 4H), 1.54−1.43 (m, 6H), 1.36 (d, *J* = 3.4 Hz, 9H), 1.17 (dd, *J* = 6.9, 3.2 Hz, 6H). ^{13}C NMR (126 MHz, Chloroform-*d*): δ 174.4, 173.8, 173.5, 156.75, 156.73, 152.3, 152.2, 148.4, 148.0, 134.7, 134.0, 129.2, 129.1, 128.0, 127.0, 126.7, 126.2, 110.2, 110.1, 109.3, 109.1, 107.6, 107.5, 81.51, 81.49, 79.3, 79.2, 53.0, 52.5, 52.2, 50.5, 50.0, 49.8, 39.1, 39.0, 34.7, 34.0, 33.79, 33.78, 28.1, 27.8, 27.7, 25.54, 25.46, 25.44, 24.4, 24.3, 24.0. MS (ESI) *m*/*z*: 509.4 $[M + H]^+$.

***tert*-Butyl 2-(3-(3-(ethyl(4-isopropylbenzyl)carbamoyl)-piperidin-1-yl)phenoxy)-2-methylpropanoate (34d).** ^{1}H NMR (500 MHz, Chloroform-*d*): δ 7.16−7.04 (m, 3H), 7.04−6.87 (m, 2H), 6.54−6.27 (m, 2H), 6.21 (ddd, *J* = 19.7, 7.9, 2.2 Hz, 1H), 4.62−4.31 (m, 2H), 3.75−3.49 (m, 2H), 3.42−3.16 (m, 2H), 3.03−2.52 (m, 4H), 1.96−1.57 (m, 4H), 1.50−1.41 (m, 6H), 1.35 (d, *J* = 3.3 Hz, 9H), 1.16 (dd, *J* = 6.9, 3.5 Hz, 6H), 1.05 (dt, *J* = 25.1, 7.1 Hz, 3H). ^{13}C NMR (126 MHz, Chloroform-*d*): δ 174.0, 173.8, 173.51, 173.48, 156.8, 156.7, 152.4, 152.3, 148.3, 147.9, 135.2, 134.4, 129.2, 129.1, 127.9, 126.9, 126.6, 126.2, 110.2, 110.1, 109.2, 109.0, 107.6, 107.4, 81.48, 81.47, 79.24, 79.21, 52.6, 52.5, 50.1, 50.0, 49.8, 47.3, 41.4, 40.8, 39.2, 39.1, 33.78, 33.76, 28.3, 28.1, 27.8, 25.55, 25.53, 25.48, 25.44, 24.5, 24.3, 24.0, 14.4, 12.7. MS (ESI) *m*/*z*: 523.4 $[M + H]^+$.

***tert*-Butyl (*R*)-2-(3-(3-(isopropyl(4-isopropylbenzyl)-carbamoyl)piperidin-1-yl)phenoxy)-2-methylpropanoate (34e).** ^{1}H NMR (500 MHz, Chloroform-*d*): δ 7.19 (d, *J* = 8.2 Hz, 1H), 7.15−7.04 (m, 3H), 6.98 (t, *J* = 8.2 Hz, 1H), 6.63−6.21 (m, 3H), 5.07−4.21 (m, 3H), 3.71 (ddt, *J* = 16.2, 12.0, 2.0 Hz, 1H), 3.57 (td, *J* = 9.8, 7.6, 3.0 Hz, 1H), 3.18−2.56 (m, 4H), 2.05−1.63 (m, 4H), 1.59−1.52 (m, 6H), 1.43 (d, *J* = 7.8 Hz, 9H), 1.33−1.00 (m, 12H). ^{13}C NMR (126 MHz, Chloroform-*d*): δ 175.2, 173.2, 172.1, 156.7, 156.5, 148.2, 147.3, 136.0, 135.3, 130.7, 130.5, 126.8, 126.49, 126.47, 126.2, 113.7, 113.4, 112.1, 111.6, 80.2, 80.0, 56.5, 56.1, 55.8, 54.9, 49.2, 46.4, 46.1, 43.9, 38.7, 37.3, 33.70, 33.68, 26.3, 25.8, 25.24, 25.18, 25.0, 24.9, 24.0, 23.9, 22.9, 22.7, 21.8, 21.7, 20.5, 20.2. MS (ESI) *m*/*z*: 537.4 $[M + H]^+$.

***tert*-Butyl (*R*)-2-(3-(3-(cyclopropyl(4-isopropylbenzyl)-carbamoyl)piperidin-1-yl)phenoxy)-2-methylpropanoate (34f).** ^{1}H NMR (500 MHz, Chloroform-*d*): δ 7.20−7.12 (m, 4H), 7.07 (t, *J* = 8.2 Hz, 1H), 6.55 (dd, *J* = 8.2, 2.3 Hz, 1H), 6.49 (t, *J* = 2.4 Hz, 1H), 6.30 (dd, *J* = 8.1, 2.3 Hz, 1H), 4.71−4.37 (m, 2H), 3.85−3.61 (m, 2H), 3.43 (ddt, *J* = 11.0, 7.1, 3.4 Hz, 1H), 2.99 (dd, *J* = 12.4, 10.9 Hz, 1H), 2.88 (p, *J* = 6.9 Hz, 1H), 2.77 (td, *J* = 12.1, 2.6 Hz, 1H), 2.59 (tt, *J* = 6.9, 4.1 Hz, 1H), 2.00−1.89 (m, 1H), 1.88−1.65 (m, 3H), 1.55 (s, 6H), 1.44 (s, 9H), 1.24 (d, *J* = 6.9 Hz, 6H), 0.97−0.75 (m, 4H). ^{13}C NMR (126 MHz, Chloroform-*d*): δ 176.8, 173.5, 156.7, 152.4, 147.6, 135.7, 129.1, 127.6, 126.6, 110.2, 109.1, 107.6, 81.5, 79.2, 52.2, 50.0, 49.5, 39.9, 33.8, 29.7, 27.8, 25.53, 25.48, 24.5, 24.0, 9.4, 9.1. MS (ESI) *m*/*z*: 535.4 $[M + H]^+$.

***N*-(4-Bromobenzyl)cyclopropanamine (35).** ^{1}H NMR (500 MHz, Chloroform-*d*): δ 7.46−7.37 (m, 2H), 7.22−7.08 (m, 2H), 3.79 (s, 2H), 2.12 (tt, *J* = 6.5, 3.6 Hz, 1H), 0.49−0.39 (m, 2H), 0.39−0.25 (m, 2H). MS (ESI) *m*/*z*: 226.0, 228.0 $[M + H]^+$.

Ethyl 1-(3-((1-(*tert*-butoxy)-2-methyl-1-oxopropan-2-yl)-oxy)phenyl)piperidine-3-carboxylate (36). ^{1}H NMR (500 MHz, Chloroform-*d*): δ 7.04 (t, *J* = 8.2 Hz, 1H), 6.54 (dd, *J* = 8.1, 2.3 Hz, 1H), 6.45 (t, *J* = 2.4 Hz, 1H), 6.31−6.21 (m, 1H), 4.12 (q, *J* = 7.1 Hz, 2H), 3.67 (ddt, *J* = 12.4, 3.5, 1.5 Hz, 1H), 3.42 (ddd, *J* = 12.3, 4.9, 3.1 Hz, 1H), 2.95 (dd, *J* = 12.4, 9.9 Hz, 1H), 2.80−2.68 (m, 1H), 2.60 (tt, *J* = 10.0, 3.9 Hz, 1H), 2.05−1.93 (m, 1H), 1.74 (th, *J* = 9.2, 3.1 Hz, 1H), 1.69−1.59 (m, 2H), 1.53 (s, 6H), 1.41 (s, 9H), 1.24 (t, *J* = 7.2 Hz, 3H). MS (ESI) *m*/*z*: 392.3 $[M + H]^+$, 414.3 $[M + Na]^+$.

***tert*-Butyl 2-(3-(3-((4-bromobenzyl)(cyclopropyl)-carbamoyl)piperidin-1-yl)phenoxy)-2-methylpropanoate (37).** ^{1}H NMR (500 MHz, Chloroform-*d*): δ 7.42 (d, *J* = 8.3 Hz, 2H), 7.11 (d, *J* = 8.3 Hz, 2H), 7.07 (t, *J* = 8.2 Hz, 1H), 6.54 (d, *J* = 8.2 Hz, 1H), 6.48 (s, 1H), 6.30 (d, *J* = 8.1 Hz, 1H), 4.59 (d, *J* = 14.7 Hz, 1H), 4.49 (d, *J* = 14.7 Hz, 1H), 3.67 (d, *J* = 12.1 Hz, 2H), 3.42 (s, 1H), 2.97 (t, *J* = 11.6 Hz, 1H), 2.76 (t, *J* = 11.0 Hz, 1H), 2.58 (s, 1H), 1.91 (d, *J* = 8.5 Hz, 1H), 1.76 (dt, *J* = 32.5, 8.6 Hz, 3H), 1.55 (d, *J* = 1.9 Hz, 6H), 1.43 (d, *J* = 2.0 Hz, 9H), 0.91−0.74 (m, 4H). MS (ESI) *m*/*z*: 571.2, 573.2 $[M + H]^+$.

***tert*-Butyl 2-(3-(3-((4-(1*H*-pyrazol-4-yl)benzyl)(cyclopropyl)-carbamoyl)piperidin-1-yl)phenoxy)-2-methylpropanoate (38a).** ^{1}H NMR (500 MHz, Chloroform-*d*): δ 7.78 (s, 2H), 7.42 (d, *J* = 8.1 Hz, 2H), 7.20 (d, *J* = 8.1 Hz, 2H), 7.07 (t, *J* = 8.2 Hz, 1H), 6.56 (d, *J* = 8.2 Hz, 1H), 6.49 (t, *J* = 2.2 Hz, 1H), 6.30 (d, *J* = 8.1 Hz, 1H), 4.67 (d, *J* = 14.7 Hz, 1H), 4.55 (d, *J* = 14.8 Hz, 1H), 3.69 (t, *J* = 11.3 Hz, 2H), 3.46 (t, *J* = 10.9 Hz, 1H), 3.04−2.97 (m, 1H), 2.77 (t, *J* = 11.0 Hz, 1H), 2.62 (dt, *J* = 6.6, 2.8 Hz, 1H), 1.94 (d, *J* = 10.6 Hz, 1H), 1.83−1.67 (m, 3H), 1.55 (s, 6H), 1.43 (s, 9H), 0.89−0.81 (m, 4H). MS (ESI) *m*/*z*: 559.4 $[M + H]^+$.

***tert*-Butyl 2-(3-(3-(cyclopropyl(4-(1-methyl-1*H*-pyrazol-4-yl)benzyl)carbamoyl)piperidin-1-yl)phenoxy)-2-methylpropanoate (38b).** ^{1}H NMR (500 MHz, Chloroform-*d*): δ 7.50 (s, 1H), 7.36 (d, *J* = 8.0 Hz, 2H), 7.29 (d, *J* = 7.8 Hz, 2H), 7.07 (t, *J* = 8.2 Hz, 1H), 6.55 (d, *J* = 8.0 Hz, 1H), 6.49 (s, 1H), 6.29 (d, *J* = 8.0 Hz, 2H), 4.65 (q, *J* = 15.0 Hz, 2H), 3.88 (s, 3H), 3.76−3.64 (m, 2H), 3.46 (t, *J* = 10.5 Hz, 1H), 2.99 (t, *J* = 11.5 Hz, 1H), 2.77 (t, *J* = 11.7 Hz, 1H), 2.69−2.65 (m, 1H), 1.95 (d, *J* = 11.0 Hz, 1H), 1.82−1.70 (m, 3H), 1.54 (s, 6H), 1.43 (s, 9H), 0.94−0.79 (m, 4H). MS (ESI) *m*/*z*: 573.4 $[M + H]^+$, 595.4 $[M + Na]^+$.

***tert*-Butyl 2-(3-(3-((4-(1*H*-pyrazol-5-yl)benzyl)(cyclopropyl)-carbamoyl)piperidin-1-yl)phenoxy)-2-methylpropanoate (38c).** ^{1}H NMR (500 MHz, Chloroform-*d*): δ 7.71 (d, *J* = 8.0 Hz, 2H), 7.65 (d, *J* = 1.4 Hz, 2H), 7.24 (d, *J* = 8.1 Hz, 2H), 7.06 (t, *J* = 8.2 Hz, 1H), 6.59−6.51 (m, 2H), 6.48 (t, *J* = 2.2 Hz, 1H), 6.29 (d, *J* = 8.1 Hz, 1H), 4.69 (d, *J* = 14.7 Hz, 1H), 4.54 (d, *J* = 14.7 Hz, 1H), 3.68 (t, *J* = 9.5 Hz, 2H), 3.44 (t, *J* = 10.9 Hz, 1H), 3.05−2.96 (m, 1H), 2.77 (t, *J* = 11.9 Hz, 1H), 2.63−2.54 (m, 1H), 1.93 (d, *J* = 10.7 Hz, 1H), 1.75 (ddd, *J* = 29.2, 17.1, 8.6 Hz, 3H), 1.54 (s, 6H), 1.42 (s, 9H), 0.88−0.78 (m, 4H). MS (ESI) *m*/*z*: 559.4 $[M + H]^+$.

***tert*-Butyl 2-(3-(3-(cyclopropyl(4-(1-methyl-1*H*-pyrazol-5-yl)benzyl)carbamoyl)piperidin-1-yl)phenoxy)-2-methylpropanoate (38d).** ^{1}H NMR (500 MHz, Chloroform-*d*): δ 7.72 (s, 1H), 7.57 (s, 1H), 7.39 (d, *J* = 7.9 Hz, 2H), 7.20 (d, *J* = 7.8 Hz, 2H), 7.05 (t, *J* = 8.2 Hz, 1H), 6.54 (d, *J* = 8.2 Hz, 1H), 6.47 (s, 1H), 6.28 (d, *J* = 8.0 Hz, 1H), 4.63 (d, *J* = 14.6 Hz, 1H), 4.56−4.51 (m, 1H), 3.90−3.88 (m, 3H), 3.71−3.63 (m, 2H), 3.41 (d, *J* = 10.7 Hz, 1H), 2.98 (t, *J* = 11.7 Hz, 1H), 2.75 (t, *J* = 11.4 Hz, 1H), 2.61−2.55 (m, 1H), 1.92 (d, *J* = 10.8 Hz, 1H), 1.74 (dq, *J* = 26.8, 15.7, 11.2 Hz, 3H), 1.53 (s, 6H), 1.41 (d, *J* = 1.2 Hz, 9H), 0.83 (ddd, *J* = 25.3, 13.1, 8.0 Hz, 4H). MS (ESI) *m*/*z*: 573.4 $[M + H]^+$.

***tert*-Butyl 2-(3-(3-(cyclopropyl(4-(thiophen-2-yl)benzyl)-carbamoyl)piperidin-1-yl)phenoxy)-2-methylpropanoate (38e).** ^{1}H NMR (500 MHz, Chloroform-*d*): δ 7.50−7.43 (m, 2H), 7.19 (dd, *J* = 3.6, 1.2 Hz, 1H), 7.18 (s, 3H), 7.02−6.92 (m, 2H), 6.47 (dd, *J* = 8.3, 2.3 Hz, 1H), 6.41 (t, *J* = 2.4 Hz, 1H), 6.22 (dd, *J* = 8.1, 2.2 Hz, 1H), 4.58 (d, *J* = 14.7 Hz, 1H), 4.47 (d, *J* = 14.7 Hz, 1H), 3.66−3.55 (m, 2H), 3.36 (tt, *J* = 10.9, 3.4 Hz, 1H), 2.92 (dd, *J* = 12.5, 10.9 Hz, 1H), 2.68 (td, *J* = 12.1, 2.7 Hz, 1H), 2.52 (tt, *J* = 6.9, 4.1 Hz, 1H), 1.89−1.83 (m, 1H), 1.74−1.59 (m, 3H), 1.46 (s, 6H), 1.34 (s, 9H), 0.83−0.65 (m, 4H). MS (ESI) *m*/*z*: 575.4 $[M + H]^+$.

***tert*-Butyl 2-(3-(3-(cyclopropyl(4-(thiophen-3-yl)benzyl)-carbamoyl)piperidin-1-yl)phenoxy)-2-methylpropanoate (38f).** ^{1}H NMR (500 MHz, Chloroform-*d*): δ 7.47−7.40 (m, 2H), 7.32 (dd, *J* = 2.6, 1.7 Hz, 1H), 7.29−7.22 (m, 2H), 7.19−7.10 (m, 2H), 6.97 (t, *J* = 8.2 Hz, 1H), 6.45 (dd, *J* = 8.2, 2.3 Hz, 1H), 6.39 (t, *J* = 2.4 Hz, 1H), 6.20 (dd, *J* = 8.0, 2.2 Hz, 1H), 4.57 (d, *J* = 14.6 Hz, 1H), 4.47 (d, *J* = 14.8 Hz, 1H), 3.64−3.53 (m, 2H), 3.34 (tt, *J* = 11.2, 3.4 Hz, 1H), 2.90 (dd, *J* = 12.5, 10.9 Hz, 1H), 2.67 (td, *J* = 12.1, 2.7 Hz, 1H), 2.51 (tt, *J* = 6.9, 4.1 Hz, 1H), 1.88−1.80 (m, 1H), 1.73−1.57 (m, 3H), 1.44 (s, 6H), 1.33 (s, 9H), 0.81−0.66 (m, 4H). MS (ESI) *m*/*z*: 575.4 $[M + H]^+$.

***tert*-Butyl 2-(3-(3-(cyclopropyl(4-(furan-2-yl)benzyl)-carbamoyl)piperidin-1-yl)phenoxy)-2-methylpropanoate (38g).** ^{1}H NMR (500 MHz, Chloroform-*d*): δ 7.58−7.50 (m, 2H), 7.37 (d, *J* = 1.7 Hz, 1H), 7.21−7.15 (m, 2H), 6.99 (t, *J* = 8.2 Hz, 1H), 6.57−6.51 (m, 1H), 6.48 (dd, *J* = 8.2, 2.3 Hz, 1H), 6.41 (t, *J* = 2.3 Hz, 1H), 6.37 (dd, *J* = 3.4, 1.8 Hz, 1H), 6.22 (dd, *J* = 8.1, 2.2 Hz, 1H), 4.59 (d, *J* = 14.7 Hz, 1H), 4.47 (d, *J* = 14.7 Hz, 1H), 3.65−3.56 (m, 2H), 3.36 (tt, *J* = 11.1, 3.5 Hz, 1H), 2.92 (dd, *J* = 12.5, 10.9 Hz, 1H), 2.69 (td, *J* =

https://doi.org/10.1021/acs.jmedchem.1c00046
J. Med. Chem. 2021, 64, 5886−5904

12.1, 2.7 Hz, 1H), 2.51 (tt, J = 6.9, 4.1 Hz, 1H), 1.90−1.81 (m, 1H), 1.76−1.61 (m, 3H), 1.47 (s, 6H), 1.35 (s, 9H), 0.82−0.69 (m, 4H). MS (ESI) m/z: 559.4 $[M + H]^+$.

***tert*-Butyl 2-(3-(3-(cyclopropyl(4-(furan-3-yl)benzyl)-carbamoyl)piperidin-1-yl)phenoxy)-2-methylpropanoate (38h).** ^{1}H NMR (500 MHz, Chloroform-*d*): δ 7.74 (t, J = 1.2 Hz, 1H), 7.52−7.42 (m, 3H), 7.27 (dd, J = 8.9, 7.0 Hz, 2H), 7.09 (t, J = 8.2 Hz, 1H), 6.71 (dd, J = 1.9, 0.9 Hz, 1H), 6.58 (dd, J = 8.2, 2.3 Hz, 1H), 6.52 (t, J = 2.3 Hz, 1H), 6.33 (dd, J = 8.1, 2.3 Hz, 1H), 4.68 (d, J = 14.7 Hz, 1H), 4.59 (d, J = 14.7 Hz, 1H), 3.78−3.67 (m, 2H), 3.47 (tt, J = 11.2, 3.6 Hz, 1H), 3.03 (dd, J = 12.5, 10.9 Hz, 1H), 2.80 (td, J = 12.1, 2.8 Hz, 1H), 2.63 (tt, J = 6.9, 4.1 Hz, 1H), 2.00−1.90 (m, 1H), 1.86−1.72 (m, 3H), 1.57 (s, 6H), 1.46 (s, 9H), 0.92−0.80 (m, 4H). MS (ESI) m/z: 559.4 $[M + H]^+$.

Ethyl (*R*)-1-(3-((1-(*tert*-butoxy)-2-methyl-1-oxopropan-2-yl)-oxy)phenyl)piperidine-3-carboxylate (39). ^{1}H NMR (500 MHz, Chloroform-*d*): δ 7.04 (t, J = 8.2 Hz, 1H), 6.54 (dd, J = 8.1, 2.3 Hz, 1H), 6.45 (t, J = 2.4 Hz, 1H), 6.31−6.21 (m, 1H), 4.12 (q, J = 7.1 Hz, 2H), 3.67 (ddt, J = 12.4, 3.5, 1.5 Hz, 1H), 3.42 (ddd, J = 12.3, 4.9, 3.1 Hz, 1H), 2.95 (dd, J = 12.4, 9.9 Hz, 1H), 2.80−2.68 (m, 1H), 2.60 (tt, J = 10.0, 3.9 Hz, 1H), 2.05−1.93 (m, 1H), 1.74 (th, J = 9.2, 3.1 Hz, 1H), 1.69−1.59 (m, 2H), 1.53 (s, 6H), 1.41 (s, 9H), 1.24 (t, J = 7.2 Hz, 3H). ^{13}C NMR (126 MHz, Chloroform-*d*): δ 173.7, 173.4, 156.6, 152.5, 129.1, 110.4, 109.3, 107.6, 81.4, 79.1, 60.4, 52.0, 49.7, 41.3, 27.8, 27.0, 25.5, 25.4, 24.1, 14.2. MS (ESI) m/z: 392.3 $[M + H]^+$, 414.3 $[M + Na]^+$.

***tert*-Butyl (*R*)-2-(3-(3-((4-bromobenzyl)(cyclopropyl)-carbamoyl)piperidin-1-yl)phenoxy)-2-methylpropanoate (40).** ^{1}H NMR (500 MHz, Chloroform-*d*): δ 7.46−7.39 (m, 2H), 7.13−7.03 (m, 3H), 6.54 (dd, J = 8.3, 2.3 Hz, 1H), 6.47 (t, J = 2.3 Hz, 1H), 6.29 (dd, J = 8.0, 2.2 Hz, 1H), 4.59 (d, J = 14.7 Hz, 1H), 4.49 (d, J = 14.7 Hz, 1H), 3.72−3.60 (m, 2H), 3.41 (tt, J = 11.0, 3.5 Hz, 1H), 2.96 (dd, J = 12.5, 10.9 Hz, 1H), 2.76 (td, J = 12.0, 2.9 Hz, 1H), 2.58 (tt, J = 7.0, 4.0 Hz, 1H), 1.94−1.89 (m, 1H), 1.79 (ddd, J = 12.4, 6.7, 3.4 Hz, 1H), 1.77−1.67 (m, 2H), 1.55 (s, 6H), 1.43 (s, 9H), 0.91−0.75 (m, 4H). MS (ESI) m/z: 571.2, 573.2 $[M + H]^+$.

***tert*-Butyl (*R*)-2-(3-(3-(cyclopropyl(4-(thiophen-2-yl)benzyl)-carbamoyl)piperidin-1-yl)phenoxy)-2-methylpropanoate (41).** ^{1}H NMR (500 MHz, Chloroform-*d*): δ 7.53−7.42 (m, 2H), 7.24−7.12 (m, 4H), 7.04−6.93 (m, 2H), 6.48 (dd, J = 8.2, 2.3 Hz, 1H), 6.41 (t, J = 2.3 Hz, 1H), 6.22 (dd, J = 8.1, 2.3 Hz, 1H), 4.59 (d, J = 14.7 Hz, 1H), 4.48 (d, J = 14.7 Hz, 1H), 3.69−3.51 (m, 2H), 3.37 (tt, J = 10.9, 3.0 Hz, 1H), 2.99−2.82 (m, 1H), 2.70 (td, J = 12.2, 2.8 Hz, 1H), 2.59−2.44 (m, 1H), 1.86 (d, J = 11.3 Hz, 1H), 1.75−1.63 (m, 3H), 1.47 (s, 6H), 1.35 (s, 9H), 0.85−0.66 (m, 4H). MS (ESI) m/z: 575.4 $[M + H]^+$.

Ethyl (*S*)-1-(3-((1-(*tert*-butoxy)-2-methyl-1-oxopropan-2-yl)-oxy)phenyl)piperidine-3-carboxylate (42). ^{1}H NMR (500 MHz, Chloroform-*d*): δ 7.07 (t, J = 8.2 Hz, 1H), 6.57 (ddd, J = 8.3, 2.4, 0.8 Hz, 1H), 6.48 (t, J = 2.4 Hz, 1H), 6.30 (ddd, J = 8.1, 2.3, 0.8 Hz, 1H), 4.20−4.11 (m, 2H), 3.70 (ddt, J = 12.3, 3.5, 1.5 Hz, 1H), 3.51−3.42 (m, 1H), 2.97 (dd, J = 12.4, 10.0 Hz, 1H), 2.77 (tdd, J = 10.2, 4.5, 3.1 Hz, 1H), 2.66−2.56 (m, 1H), 2.06−1.95 (m, 1H), 1.82−1.72 (m, 1H), 1.72−1.62 (m, 2H), 1.55 (s, 6H), 1.44 (s, 9H), 1.27 (t, J = 7.1 Hz, 3H). ^{13}C NMR (126 MHz, Chloroform-*d*): δ 173.8, 173.5, 156.6, 152.5, 129.1, 110.4, 109.3, 107.6, 81.5, 79.2, 60.5, 52.1, 49.7, 41.4, 27.8, 27.0, 25.5, 25.4, 24.1, 14.3. MS (ESI) m/z: 392.2 $[M + H]^+$.

***tert*-Butyl (*S*)-2-(3-(3-((4-bromobenzyl)(cyclopropyl)-carbamoyl)piperidin-1-yl)phenoxy)-2-methylpropanoate (43).** ^{1}H NMR (500 MHz, $CDCl_3$): δ 7.37−7.33 (m, 2H), 7.08−6.91 (m, 3H), 6.47 (dd, J = 8.1, 2.4 Hz, 1H), 6.40 (t, J = 2.3 Hz, 1H), 6.27−6.03 (m, 1H), 4.52 (d, J = 14.7 Hz, 1H), 4.47 (s, 1H), 3.63−3.51 (m, 2H), 3.34 (tt, J = 10.8, 3.5 Hz, 1H), 2.90 (dd, J = 12.5, 10.9 Hz, 1H), 2.69 (td, J = 12.1, 2.8 Hz, 1H), 2.51 (tt, J = 6.9, 4.1 Hz, 1H), 1.84−1.62 (m, 4H), 1.48 (s, 6H), 1.36 (s, 9H), 0.85−0.65 (m, 4H). MS (ESI) m/z: 571.2, 573.2 $[M + H]^+$.

***tert*-Butyl (*S*)-2-(3-(3-(cyclopropyl(4-(thiophen-2-yl)benzyl)-carbamoyl)piperidin-1-yl)phenoxy)-2-methylpropanoate (44).** ^{1}H NMR (500 MHz, $CDCl_3$): δ 7.61−7.43 (m, 2H), 7.31−7.19 (m, 4H), 7.10−7.00 (m, 2H), 6.56 (dd, J = 7.9, 2.3 Hz, 1H), 6.49 (t, J = 2.3 Hz, 1H), 6.33−6.15 (m, 1H), 4.67 (d, J = 14.7 Hz, 1H), 4.56 (d, J = 14.7 Hz, 1H), 3.77−3.60 (m, 2H), 3.45 (tt, J = 11.0, 3.5 Hz, 1H), 3.00 (dd, J = 12.4, 11.0 Hz, 1H), 2.77 (td, J = 12.2, 2.8 Hz, 1H), 2.70−2.45 (m, 1H), 2.01−1.87 (m, 1H), 1.83−1.74 (m, 2H), 1.55 (s, 6H), 1.43 (s, 9H), 0.97−0.73 (m, 4H). MS (ESI) m/z: 575.3 $[M + H]^+$.

Protein Expression and Purification. Full-length β-catenin (residues 1−781) was cloned into a pET-28b vector carrying a *C*-terminal 6× histidine (Novagen) and transformed into *Escherichia coli* BL21 DE3 (Novagen). Cells were cultured in LB medium with 50 μg/mL kanamycin until the OD_{600} was approximately 0.8, and then, protein expression was induced with 400 μM IPTG at 20 °C overnight. Cells were lysed by sonication. The proteins were purified by three steps of chromatography, including Ni-NTA affinity chromatography (30210, Qiagen), HiTrap Q HP anion exchange chromatography (17-1154-01, GE Healthcare Life Science), and size-exclusion chromatography with a HiLoad 26/600 Superdex 200 pg column (28-9893-36, GE Healthcare Life Science) using an AKTA Pure FPLC (GE Healthcare Life Science) system. Protein was eluted in a buffer containing 20 mM Tris (pH 8.5), 100 mM NaCl, and 2 mM DTT. The purity of β-catenin was greater than 95% as determined by SDS-PAGE gel analyses. Thermal shift assays were performed on a CFX96 real-time system (Bio-Rad) to monitor protein stability and detect protein aggregation. Protein unfolding was evaluated through measurement of the fluorescence changes of fluorescent dye Sypro Orange when interacting with β-catenin proteins. A temperature increment of 1°/min was applied. All proteins were stable, and no aggregation was observed under storage or assay conditions. Proteins were aliquoted and stored at −80 °C.

BCL9 Peptide Synthesis and Purification. Human BCL9 (residues 350−375) and *N*-terminally biotinylated human BCL9 (residues 350−375) were synthesized by InnoPep Inc. (San Diego, CA, www.innopep.com). The synthesized peptides were purified by HPLC with purity >95%. The structures were validated by LC/MS. The sequences of the peptides are provided in Table 6.

Table 6. Sequences of Peptides

peptide	sequence[a]
BCL9 26-mer	H-^{350}GLSQEQLEHRERSLQTLRDIQRMLFP^{375}-NH_2
biotinylated BCL9 26-mer	biotin-Ahx-^{350}GLSQEQLEHRERSLQTLRDIQRMLFP^{375}-NH_2

[a]Ahx, 6-aminohexanoic acid.

AlphaScreen Assays of β-Catenin and BCL9 Interaction. Experiments were performed in white opaque 384-well plates from PerkinElmer (Waltham, MA), and the samples were read on a Biotek Synergy 2 plate reader (Winooski, VT) with excitation at 680 nm and emission at 570 nm. The standard AlphaScreen protocol was used with a sensitivity setting of 200. All dilutions were made in 1× assay buffer containing 25 mM Hepes (pH 7.4), 100 mM NaCl, 0.01% Triton X-100, and 0.1% BSA to minimize nonspecific interactions. For the competitive inhibition assays of the β-catenin/BCL9 PPI, the negative control (equivalent to 0% inhibition) refers to 5.0 nM biotinylated BCL9, 50 nM His_6-tagged β-catenin, and 10 μg/mL donor and acceptor beads in a final volume of 25 μL assay buffer, with no tested inhibitor present. The positive control (equivalent to 100% inhibition) refers to 5.0 nM biotinylated BCL9 and 10 μg/mL donor and acceptor beads in a final volume of 25 μL assay buffer.

For the β-catenin/BCL9 assay, 5 nM biotinylated BCL9 and 50 nM His_6-tagged β-catenin were incubated in assay buffer for 30 min. Different concentrations of the tested inhibitor were added and incubated in 20 μL assay buffer for another 1 h. All of the assay plates were covered and gently mixed on an orbital shaker. Donor and acceptor beads were then added to the plates to a final concentration of 10 μg/mL in 25 μL of assay buffer. The mixture was incubated for 1 h before detection. The IC_{50} value was determined by nonlinear least-square analysis of GraphPad Prism 8.0. The K_i values were derived from the IC_{50} values using a method reported by Wang and co-workers.[60] The equation used is $K_i = [I]_{50}/([L]_{50}/K_d + [P]_0/K_d + 1)$ (where $[I]_{50}$ denotes the concentration of the free inhibitor at 50% inhibition, $[L]_{50}$

https://doi.org/10.1021/acs.jmedchem.1c00046
J. Med. Chem. 2021, 64, 5886−5904

is the concentration of the free labeled ligand at 50% inhibition, $[P]_0$ is the concentration of the free protein at 0% inhibition, and K_d is the dissociation constant of the protein−ligand complex). All of the experiments were performed in triplicate and carried out in the presence of 1% DMSO for small-molecule inhibitors. Each compound was assayed at least by three independent experiments. The results were expressed as mean ± standard deviation.

co-IP Experiments. Colorectal cancer HCT116 cells with hyperactive β-catenin signaling at 1× 10^6 cells/mL were treated with different concentrations of the inhibitor for 24 h. Cells were then lysed in buffer containing 50 mM Tris, pH 7.4, 150 mM NaCl, 1% Nonidet P-40, 2 mM EDTA, and protease inhibitors. The cell lysates were pre-adsorbed to A/G plus agarose (sc-2003, Santa Cruz Biotechnology) at 4 °C for 1 h. Pre-adsorbed lysates were incubated with a specific primary antibody against β-catenin (610153, BD Biosciences) overnight at 4 °C. A/G plus agarose was then added to the lysate mixture and incubated for 3 h. The beads were washed four times with the lysis buffer at 4 °C. The bound protein was eluted by boiling in the SDS sample buffer and loaded onto 8% SDS polyacrylamide gel for electrophoretic analysis. Separated proteins were transferred onto nitrocellulose membranes for immunoblot analysis. The antibodies against BCL9 (ab37305, Abcam) and E-cadherin (610404, BD Biosciences) were incubated with the membranes. IRDye 680LT goat anti-mouse IgG (827-11080, LiCOR) and IRDye 800CW goat anti-rabbit IgG (926-32211, LiCOR) were used as the secondary antibodies. The images were detected using the Odyssey infrared imaging system (LiCOR). Experiments were performed in triplicate.

Cell Transfection and Luciferase Assay. The FuGENE6 (E269A, Promega) 96-well plate format was used for the transfection of colorectal cancer SW480 cells according to the manufacturer's instruction. SW480 cells were co-transfected with 60 ng of TOPFlash or FOPFlash firefly luciferase reporter gene and 40 ng of renilla luciferase pCMV-RL normalization reporter gene. Cells were cultured in Dulbecco's modified Eagle medium (DMEM) and 10% fetal bovine serum (FBS) at 37 °C for 24 h. Different concentrations of inhibitors or DMSO were added and incubated in DMEM with 5% FBS. After 24 h, the luciferase reporter activity was measured using the Dual-Glo system (E2940, Promega). Normalized luciferase activity in response to the treatment with inhibitors was compared with that obtained from the cells treated with DMSO. Experiments were performed in triplicate.

Quantitative Real-Time PCR Analysis. SW480 cells at 1× 10^6 cells/mL were treated with inhibitors at different concentrations for 24 h. MDA-MB-231 cells at 1 × 10^6 cells/mL were treated with 100 ng/mL recombinant Wnt 3a (rmW3aL-010, Time BioScience) for 30 min; then, the inhibitors at different concentrations were added and incubated for 24 h. Total RNAs were extracted with TRIzol (15596026, Life Technologies), and the cDNA was synthesized with the superscript III first-strand kit (18080-051, Invitrogen). qPCR experiments were performed using the iQTM SYBR green supermix kit (170-8880, BIO-RAD) on an CFX96 real-time system (BIO-RAD). The threshold cycle (CT) values were normalized to those of internal reference GAPDH. Experiments were performed in triplicate. The primer pairs are shown in Table 7.

Table 7. Primer Pairs

human *GAPDH*	forward	5′-GAAGGTGAAGGTCGGAGTC-3′
	reverse	5′-GAAGATGGTGATGGGATTTC-3′
human HPRT	forward	5′-GCTATAAATTCTTTGCTGACCTGC TG-3′
	reverse	5′-AATTACTTTTATGTCCCCTGTTGA CTGG-3′
human AXIN2	forward	5′-AGTGTGAGGTCCACGGAAAC-3′
	reverse	5′-CTTCACACTGCGATGCATTT-3′
human LEF1	forward	5′-GACGAGATGATCCCCTTCAA-3′
	reverse	5′-AGGGCTCCTGAGAGGTTTGT-3′
human cyclin D1	forward	5′-ACAAACAGATCATCCGCAAACAC-3′
	reverse	5′-TGTTGGGGCTCCTCAGGTTC-3′

Western Blotting of Wnt Target Genes. SW480 cells at 1 × 10^6 cells/mL were treated with different concentrations of inhibitors for 24 h. Cells were lysed in buffer containing 50 mM Tris, pH 7.4, 150 mM NaCl, 1% Nonidet P-40, 2 mM EDTA, and protease inhibitors. After centrifugation at 12,000 rpm for 20 min at 4 °C, the supernatant was loaded onto an 8% SDS polyacrylamide gel for electrophoretic analysis. Separated proteins were transferred onto nitrocellulose membranes for immunoblot analysis. The antibodies against Axin2 (MA5-15015, Thermo Fisher), cyclin D1 (sc-853, Santa Cruz Biotechnology), and β-tubulin (sc-55529, Santa Cruz Biotechnology) were incubated with the membranes overnight at 4 °C. IRDye 680LT goat anti-mouse IgG (827-11080, LiCOR) or IRDye 800CW goat anti-rabbit IgG (827-08365, LiCOR) was used as the secondary antibody. The images were detected using the Odyssey infrared imaging system (Odyssey Fc, LiCOR). Experiments were performed in triplicate.

MTS Cell Growth Inhibition Experiments. Colorectal cancer cells (SW480 and HCT116) and triple negative breast cancer cells (MDA-MB-231 and MDA-MB-468) were seeded in 96-well plates at 5 × 10^3 cells/well in DMEM with 10% FBS, maintained overnight at 37 °C, and then incubated with the tested compounds at various concentrations in DMEM with 5% FBS. Human mammary epithelial MCF10A cells were seeded in 96-well plates at 1 × 10^4 cells/well in mammary epithelial cell growth medium (MEGM) (CC-3150, Lonza) with 100 ng/mL cholera toxin, maintained overnight at 37 °C, and incubated with the tested compounds at various concentrations. Cell viability was monitored after 72 h using a freshly prepared mixture of one part phenazine methosulfate (PMS, Sigma) solution (0.92 mg/mL) and 19 parts 3-(4,5-dimethylthiazol-2-yl)-5-(3-carboxymethoxyphenyl)-2-(4-sulfophenyl)-2*H*-tetrazolium (MTS, Promega) solution (2 mg/mL). Cells were incubated in 10 μL of this solution at 37 °C for 3 h, and absorptions at 490 nm (A490) were measured. The effect of each compound is expressed as the concentration required to reduce A490 by 50% (IC_{50}) relative to DMSO-treated cells. Experiments were performed in triplicate.

Biotin Streptavidin Pull-down Assay. SW480 colon cancer cells were lysed in NP-40 buffer (50 mM Tris pH 7.4, 150 mM NaCl, 1% NP-40, and 2 mM EDTA) with protease inhibitors. Cell lysate (2 mg/mL) was precleared with streptavidin-agarose beads (S-1638, Sigma) and incubated with the indicated concentrations of the compound or BCL9 HD2 peptide (residues 350−375) for 1 h at 4 °C. Then, the cell lysate was incubated with *N*-terminally biotinylated BCL9 HD2 peptide (residues 350−375) (0.2 μM) for 2 h at 4 °C. Protein−peptide complexes were pulled down with streptavidin-agarose beads for 2 h at 4 °C. Beads were washed four times with NP-40 buffer, and protein was eluted by boiling in 4× SDS loading buffer. The samples were loaded onto 8% SDS polyacrylamide gel for electrophoretic analysis. Separated proteins were transferred onto nitrocellulose membranes for immunoblot analysis. The antibody against β-catenin (610153, BD Biosciences) was incubated with membranes. IRDye 800CW goat anti-mouse IgG (926-32210, LiCOR) was used as the secondary antibody. The images were detected using the Odyssey infrared imaging system (LiCOR). Experiments were performed in triplicate.

β-Catenin Rescue Experiments. SW480 cells were seeded in 96-well plates at 1 × 10^4 cells/well in DMEM with 10% FBS and maintained overnight at 37 °C. Then, 200 ng of pcDNA3.1−β-catenin or 200 ng of empty vector pcDNA3.1 per well was transfected into the cells, and 12 h later, the tested compound at various concentrations was added into the cells in DMEM with 5% FBS. Cell viability was monitored after 72 h using a freshly prepared mixture of one part phenazine methosulfate (PMS, Sigma) solution (0.92 mg/mL) and 19 parts MTS (Promega) solution (2 mg/mL). Cells were incubated in 10 μL of this solution at 37 °C for 3 h, and A490 was measured. The effect of each compound is expressed as the concentration required to reduce A490 by 50% (IC_{50}) relative to DMSO-treated cells. Experiments were performed in triplicate.

Docking Studies. Crystallographic coordinates for the human β-catenin armadillo repeat domain (PDB id 2GL7, 2.60 Å resolution, Rcryst = 0.223, residues 142−663) were obtained from the Research Collaboratory for Structural Bioinformatics (RCSB) Protein Data Bank (PDB). Preparation of the crystal structure and molecular modeling

https://doi.org/10.1021/acs.jmedchem.1c00046
J. Med. Chem. 2021, 64, 5886−5904

were achieved with the commercially available Schrodinger (http://www.schrodinger.com/) software packages. The protein was processed using the "Protein Preparation Wizard" workflow in Maestro 11.4 (Schrodinger LLC) to add bond orders and hydrogens. All heteroatom (het) residues and crystal water molecules beyond 5 Å from the het group were removed. Small molecules were built in the LigPrep module using the OPLS3 force field. The Glide module was used as the docking program. The standard precision (SP) approach of Glide was adopted to dock small molecules into β-catenin with the default parameters. Residues in the BCL9 L366/I369/L373 binding site of β-catenin include D144−A146, L148, A149, A152, I153, E155−L160, D162−A171, M174, V175, Q177, L178, K180, K181, A183, S184, A187, I188, M194, and I198.

■ ASSOCIATED CONTENT

Supporting Information

The Supporting Information is available free of charge at https://pubs.acs.org/doi/10.1021/acs.jmedchem.1c00046.

K_D of full-length β-catenin/BCL9 PPI; AlphaScreen assay curves of β-catenin/BCL9 inhibitors; full images of Western blot, β-catenin pull-down, and co-IP experiments; β-catenin rescue assay results of **30**; HPLC conditions and chromatograms; and NMR spectra (PDF)

Glide docking models of **29** and **30** with β-catenin (PDB)

Crystallographic coordinates (PDB)

Molecular formula strings (CSV)

■ AUTHOR INFORMATION

Corresponding Author

Haitao Ji − *Drug Discovery Department, H. Lee Moffitt Cancer Center and Research Institute, Tampa, Florida 33612-9497, United States; Departments of Oncologic Sciences and Chemistry, University of South Florida, Tampa, Florida 33620-9497, United States;* orcid.org/0000-0001-5526-4503; Phone: (813) 745-8070; Email: Haitao.Ji@moffitt.org; Fax: (813) 745-4506

Authors

Zhen Wang − *Drug Discovery Department, H. Lee Moffitt Cancer Center and Research Institute, Tampa, Florida 33612-9497, United States*

Min Zhang − *Drug Discovery Department, H. Lee Moffitt Cancer Center and Research Institute, Tampa, Florida 33612-9497, United States*

Wen Luo − *Drug Discovery Department, H. Lee Moffitt Cancer Center and Research Institute, Tampa, Florida 33612-9497, United States*

Yongqiang Zhang − *Department of Chemistry, Center for Cell and Genome Science, University of Utah, Salt Lake City, Utah 84112-0850, United States;* orcid.org/0000-0002-7210-4787

Complete contact information is available at: https://pubs.acs.org/10.1021/acs.jmedchem.1c00046

Author Contributions

‖Z.W. and M.Z. contributed equally to this work.

Notes

The authors declare the following competing financial interest(s): a provisional patent application has been filed based on these results.

■ ACKNOWLEDGMENTS

This work was supported by the Department of Defense CDMRP BCRP breakthrough award W81XWH-14-1-0083, the Susan G. Komen Career Catalyst Research Grant CCR16380693, and Floridian Breast Cancer Foundation Scientific Grant (19012901). The H. Lee Moffitt Cancer Center and Research Institute is an NCI-designated Comprehensive Cancer Center, supported under NIH grant P30-CA76292. We thank John A. Wisniewski for the initial synthesis of some compounds.

■ ABBREVIATIONS

APC, adenomatous polyposis coli; BCL9, B-cell lymphoma 9; BCL9L, BCL9-like; CBP, CREB-binding protein; CK1α, casein kinase 1α; co-IP, co-immunoprecipitation; DMEM, Dulbecco's modified Eagle medium; Dvl, Disheveled; FBS, fetal bovine serum; Fzd, Frizzled; GSK3β, glycogen synthase kinase 3β; HD2, homology domain 2; K_i, inhibition constant; LEF, lymphoid enhancer-binding factor; MEGM, mammary epithelial cell growth medium; PAINS, pan-assay interference compounds; PP2A, protein phosphatase 2A; PPI, protein−protein interaction; Pygo, Pygopus; PNPB, 3-(4-fluorophenyl)-*N*-phenylbenzamide; qPCR, quantitative real-time PCR; TCF, T-cell factor

■ REFERENCES

(1) Nusse, R.; Clevers, H. Wnt/β-catenin signaling, disease, and emerging therapeutic modalities. *Cell* **2017**, *169*, 985−999.

(2) Clevers, H.; Loh, K. M.; Nusse, R. Stem cell signaling. An integral program for tissue renewal and regeneration: Wnt signaling and stem cell control. *Science* **2014**, *346*, 1248012.

(3) Klaus, A.; Birchmeier, W. Wnt signalling and its impact on development and cancer. *Nat. Rev. Cancer* **2008**, *8*, 387−398.

(4) Polakis, P. Wnt signaling in cancer. *Cold Spring Harbor Perspect. Biol.* **2012**, *4*, a00805.

(5) Herr, P.; Hausmann, G.; Basler, K. WNT secretion and signalling in human disease. *Trends Mol. Med.* **2012**, *18*, 483−493.

(6) Anastas, J. N.; Moon, R. T. WNT signalling pathways as therapeutic targets in cancer. *Nat. Rev. Cancer* **2013**, *13*, 11−26.

(7) Bienz, M.; Clevers, H. Linking colorectal cancer to Wnt signaling. *Cell* **2000**, *103*, 311−320.

(8) Satoh, S.; Daigo, Y.; Furukawa, Y.; Kato, T.; Miwa, N.; Nishiwaki, T.; Kawasoe, T.; Ishiguro, H.; Fujita, M.; Tokino, T.; Sasaki, Y.; Imaoka, S.; Murata, M.; Shimano, T.; Yamaoka, Y.; Nakamura, Y. AXIN1 mutations in hepatocellular carcinomas, and growth suppression in cancer cells by virus-mediated transfer of AXIN1. *Nat. Genet.* **2000**, *24*, 245−250.

(9) Liu, W.; Dong, X.; Mai, M.; Seelan, R. S.; Taniguchi, K.; Krishnadath, K. K.; Halling, K. C.; Cunningham, J. M.; Qian, C.; Christensen, E.; Roche, P. C.; Smith, D. I.; Thibodeau, S. N.; Smith, D. I.; Thibodeau, S. N. Mutations in AXIN2 cause colorectal cancer with defective mismatch repair by activating β-catenin/TCF signalling. *Nat. Genet.* **2000**, *26*, 146−147.

(10) Nakajima, M.; Fukuchi, M.; Miyazaki, T.; Masuda, N.; Kato, H.; Kuwano, H. Reduced expression of Axin correlates with tumour progression of oesophageal squamous cell carcinoma. *Br. J. Cancer* **2003**, *88*, 1734−1739.

(11) Morin, P. J.; Sparks, A. B.; Korinek, V.; Barker, N.; Clevers, H.; Vogelstein, B.; Kinzler, K. W. Activation of β-catenin-Tcf signaling in colon cancer by mutations in β-catenin or APC. *Science* **1997**, *275*, 1787−1790.

(12) Coste, A. d. L.; Romagnolo, B.; Billuart, P.; Renard, C.-A.; Buendia, M.-A.; Soubrane, O.; Fabre, M.; Chelly, J.; Beldjord, C.; Kahn, A.; Perret, C. Somatic mutations of the β-catenin gene are frequent in mouse and human hepatocellular carcinomas. *Proc. Natl. Acad. Sci. U.S.A.* **1998**, *95*, 8847−8851.

(13) Robinson, D.; Van Allen, E. M.; Wu, Y.-M.; Schultz, N.; Lonigro, R. J.; Mosquera, J.-M.; Montgomery, B.; Taplin, M.-E.; Pritchard, C. C.; Attard, G.; Beltran, H.; Abida, W.; Bradley, R. K.; Vinson, J.; Cao, X.; Vats, P.; Kunju, L. P.; Hussain, M.; Feng, F. Y.; Tomlins, S. A.; Cooney, K. A.; Smith, D. C.; Brennan, C.; Siddiqui, J.; Mehra, R.; Chen, Y.; Rathkopf, D. E.; Morris, M. J.; Solomon, S. B.; Durack, J. C.; Reuter, V. E.; Gopalan, A.; Gao, J.; Loda, M.; Lis, R. T.; Bowden, M.; Balk, S. P.; Gaviola, G.; Sougnez, C.; Gupta, M.; Yu, E. Y.; Mostaghel, E. A.; Cheng, H. H.; Mulcahy, H.; True, L. D.; Plymate, S. R.; Dvinge, H.; Ferraldeschi, R.; Flohr, P.; Miranda, S.; Zafeiriou, Z.; Tunariu, N.; Mateo, J.; Perez-Lopez, R.; Demichelis, F.; Robinson, B. D.; Schiffman, M.; Nanus, D. M.; Tagawa, S. T.; Sigaras, A.; Eng, K. W.; Elemento, O.; Sboner, A.; Heath, E. I.; Scher, H. I.; Pienta, K. J.; Kantoff, P.; de Bono, J. S.; Rubin, M. A.; Nelson, P. S.; Garraway, L. A.; Sawyers, C. L.; Chinnaiyan, A. M. Integrative clinical genomics of advanced prostate cancer. *Cell* **2015**, *161*, 1215−1228.

(14) Garcia-Rostan, G.; Tallini, G.; Herrero, A.; D'Aquila, T. G.; Carcangiu, M. L.; Rimm, D. L. Frequent mutation and nuclear localization of β-catenin in anaplastic thyroid carcinoma. *Cancer Res.* **1999**, *59*, 1811−1815.

(15) Palacios, J.; Gamallo, C. Mutations in the β-catenin gene (CTNNB1) in endometrioid ovarian carcinomas. *Cancer Res.* **1998**, *58*, 1344−1347.

(16) Bafico, A.; Liu, G.; Goldin, L.; Harris, V.; Aaronson, S. A. An autocrine mechanism for constitutive Wnt pathway activation in human cancer cells. *Cancer Cell* **2004**, *6*, 497−506.

(17) Caldwell, G. M.; Jones, C.; Gensberg, K.; Jan, S.; Hardy, R. G.; Byrd, P.; Chughtai, S.; Wallis, Y.; Matthews, G. M.; Morton, D. G. The Wnt antagonist sFRP1 in colorectal tumorigenesis. *Cancer Res.* **2004**, *64*, 883−888.

(18) Suzuki, H.; Watkins, D. N.; Jair, K.-W.; Schuebel, K. E.; Markowitz, S. D.; Dong Chen, W.; Pretlow, T. P.; Yang, B.; Akiyama, Y.; Van Engeland, M.; Toyota, M.; Tokino, T.; Hinoda, Y.; Imai, K.; Herman, J. G.; Baylin, S. B. Epigenetic inactivation of SFRP genes allows constitutive WNT signaling in colorectal cancer. *Nat. Genet.* **2004**, *36*, 417−422.

(19) Fukui, T.; Kondo, M.; Ito, G.; Maeda, O.; Sato, N.; Yoshioka, H.; Yokoi, K.; Ueda, Y.; Shimokata, K.; Sekido, Y. Transcriptional silencing of secreted frizzled related protein 1 (SFRP 1) by promoter hypermethylation in non-small-cell lung cancer. *Oncogene* **2005**, *24*, 6323−6327.

(20) Milovanovic, T.; Planutis, K.; Nguyen, A.; Marsh, J. L.; Lin, F.; Hope, C.; Holcombe, R. F. Expression of Wnt genes and frizzled 1 and 2 receptors in normal breast epithelium and infiltrating breast carcinoma. *Internet J. Oncol.* **2004**, *25*, 1337−1342.

(21) Zou, H.; Molina, J. R.; Harrington, J. J.; Osborn, N. K.; Klatt, K. K.; Romero, Y.; Burgart, L. J.; Ahlquist, D. A. Aberrant methylation of secreted frizzled-related protein genes in esophageal adenocarcinoma and Barrett's esophagus. *Int. J. Cancer* **2005**, *116*, 584−591.

(22) Uematsu, K.; Kanazawa, S.; You, L.; He, B.; Xu, Z.; Li, K.; Peterlin, B. M.; McCormick, F.; Jablons, D. M. Wnt pathway activation in mesothelioma: evidence of Dishevelled overexpression and transcriptional activity of β-catenin. *Cancer Res.* **2003**, *63*, 4547−4551.

(23) Spranger, S.; Bao, R.; Gajewski, T. F. Melanoma-intrinsic β-catenin signalling prevents anti-tumour immunity. *Nature* **2015**, *523*, 231−235.

(24) Luke, J. J.; Bao, R.; Sweis, R. F.; Spranger, S.; Gajewski, T. F. WNT/β-catenin pathway activation correlates with immune exclusion across human cancers. *Clin. Cancer Res.* **2019**, *25*, 3074−3083.

(25) Grasso, C. S.; Giannakis, M.; Wells, D. K.; Hamada, T.; Mu, X. J.; Quist, M.; Nowak, J. A.; Nishihara, R.; Qian, Z. R.; Inamura, K.; Morikawa, T.; Nosho, K.; Abril-Rodriguez, G.; Connolly, C.; Escuin-Ordinas, H.; Geybels, M. S.; Grady, W. M.; Hsu, L.; Hu-Lieskovan, S.; Huyghe, J. R.; Kim, Y. J.; Krystofinski, P.; Leiserson, M. D. M.; Montoya, D. J.; Nadel, B. B.; Pellegrini, M.; Pritchard, C. C.; Puig-Saus, C.; Quist, E. H.; Raphael, B. J.; Salipante, S. J.; Shin, D. S.; Shinbrot, E.; Shirts, B.; Shukla, S.; Stanford, J. L.; Sun, W.; Tsoi, J.; Upfill-Brown, A.; Wheeler, D. A.; Wu, C. J.; Yu, M.; Zaidi, S. H.; Zaretsky, J. M.; Gabriel, S. B.; Lander, E. S.; Garraway, L. A.; Hudson, T. J.; Fuchs, C. S.; Ribas, A.; Ogino, S.; Peters, U. Genetic mechanisms of immune evasion in colorectal cancer. *Cancer Discovery* **2018**, *8*, 730−749.

(26) Spranger, S.; Dai, D.; Horton, B.; Gajewski, T. F. Tumor-residing Batf3 dendritic cells are required for effector T cell trafficking and adoptive T cell therapy. *Cancer Cell* **2017**, *31*, 711−723.

(27) Jiménez-Sánchez, A.; Memon, D.; Pourpe, S.; Veeraraghavan, H.; Li, Y.; Vargas, H. A.; Gill, M. B.; Park, K. J.; Zivanovic, O.; Konner, J.; Ricca, J.; Zamarin, D.; Walther, T.; Aghajanian, C.; Wolchok, J. D.; Sala, E.; Merghoub, T.; Snyder, A.; Miller, M. L. Heterogeneous tumor-immune microenvironments among differentially growing metastases in an ovarian cancer patient. *Cell* **2017**, *170*, 927−938.

(28) Ruiz de Galarreta, M.; Bresnahan, E.; Molina-Sánchez, P.; Lindblad, K. E.; Maier, B.; Sia, D.; Puigvehi, M.; Miguela, V.; Casanova-Acebes, M.; Dhainaut, M.; Villacorta-Martin, C.; Singhi, A. D.; Moghe, A.; von Felden, J.; Tal Grinspan, L.; Wang, S.; Kamphorst, A. O.; Monga, S. P.; Brown, B. D.; Villanueva, A.; Llovet, J. M.; Merad, M.; Lujambio, A. β-Catenin activation promotes immune escape and resistance to anti-PD-1 therapy in hepatocellular carcinoma. *Cancer Discovery* **2019**, *9*, 1124−1141.

(29) Waaler, J.; Mygland, L.; Tveita, A.; Strand, M. F.; Solberg, N. T.; Olsen, P. A.; Aizenshtadt, A.; Fauskanger, M.; Lund, K.; Brinch, S. A.; Lycke, M.; Dybing, E.; Nygaard, V.; Bøe, S. L.; Heintz, K. M.; Hovig, E.; Hammarström, C.; Corthay, A.; Krauss, S. Tankyrase inhibition sensitizes melanoma to PD-1 immune checkpoint blockade in syngeneic mouse models. *Commun. Biol.* **2020**, *3*, 196.

(30) Chen, B.; Dodge, M. E.; Tang, W.; Lu, J.; Ma, Z.; Fan, C.-W.; Wei, S.; Hao, W.; Kilgore, J.; Williams, N. S.; Roth, M. G.; Amatruda, J. F.; Chen, C.; Lum, L. Small molecule-mediated disruption of Wnt-dependent signaling in tissue regeneration and cancer. *Nat. Chem. Biol.* **2009**, *5*, 100−107.

(31) Liu, J.; Pan, S.; Hsieh, M. H.; Ng, N.; Sun, F.; Wang, T.; Kasibhatla, S.; Schuller, A. G.; Li, A. G.; Cheng, D.; Li, J.; Tompkins, C.; Pferdekamper, A.; Steffy, A.; Cheng, J.; Kowal, C.; Phung, V.; Guo, G.; Wang, Y.; Graham, M. P.; Flynn, S.; Brenner, J. C.; Li, C.; Villarroel, M. C.; Schultz, P. G.; Wu, X.; McNamara, P.; Sellers, W. R.; Petruzzelli, L.; Boral, A. L.; Seidel, H. M.; McLaughlin, M. E.; Che, J.; Carey, T. E.; Vanasse, G.; Harris, J. L. Targeting Wnt-driven cancer through the inhibition of Porcupine by LGK974. *Proc. Natl. Acad. Sci. U.S.A.* **2013**, *110*, 20224−20229.

(32) Huang, S.-M. A.; Mishina, Y. M.; Liu, S.; Cheung, A.; Stegmeier, F.; Michaud, G. A.; Charlat, O.; Wiellette, E.; Zhang, Y.; Wiessner, S.; Hild, M.; Shi, X.; Wilson, C. J.; Mickanin, C.; Myer, V.; Fazal, A.; Tomlinson, R.; Serluca, F.; Shao, W.; Cheng, H.; Shultz, M.; Rau, C.; Schirle, M.; Schlegl, J.; Ghidelli, S.; Fawell, S.; Lu, C.; Curtis, D.; Kirschner, M. W.; Lengauer, C.; Finan, P. M.; Tallarico, J. A.; Bouwmeester, T.; Porter, J. A.; Bauer, A.; Cong, F. Tankyrase inhibition stabilizes axin and antagonizes Wnt signalling. *Nature* **2009**, *461*, 614−620.

(33) Gurney, A.; Axelrod, F.; Bond, C. J.; Cain, J.; Chartier, C.; Donigan, L.; Fischer, M.; Chaudhari, A.; Ji, M.; Kapoun, A. M.; Lam, A.; Lazetic, S.; Ma, S.; Mitra, S.; Park, I.-K.; Pickell, K.; Sato, A.; Satyal, S.; Stroud, M.; Tran, H.; Yen, W.-C.; Lewicki, J.; Hoey, T. Wnt pathway inhibition via the targeting of Frizzled receptors results in decreased growth and tumorigenicity of human tumors. *Proc. Natl. Acad. Sci. U.S.A.* **2012**, *109*, 11717−11722.

(34) Thorne, C. A.; Hanson, A. J.; Schneider, J.; Tahinci, E.; Orton, D.; Cselenyi, C. S.; Jernigan, K. K.; Meyers, K. C.; Hang, B. I.; Waterson, A. G.; Kim, K.; Melancon, B.; Ghidu, V. P.; Sulikowski, G. A.; LaFleur, B.; Salic, A.; Lee, L. A.; Miller, D. M., 3rd; Lee, E. Small-molecule inhibition of Wnt signaling through activation of casein kinase 1α. *Nat. Chem. Biol.* **2010**, *6*, 829−836.

(35) Cheong, J. K.; Hung, N. T.; Wang, H.; Tan, P.; Voorhoeve, P. M.; Lee, S. H.; Virshup, D. M. IC261 induces cell cycle arrest and apoptosis of human cancer cells via CK1δ/ε and Wnt/β-catenin independent inhibition of mitotic spindle formation. *Oncogene* **2011**, *30*, 2558−2569.

(36) Mani, M.; Carrasco, D. E.; Zhang, Y.; Takada, K.; Gatt, M. E.; Dutta-Simmons, J.; Ikeda, H.; Diaz-Griffero, F.; Pena-Cruz, V.; Bertagnolli, M.; Myeroff, L. L.; Markowitz, S. D.; Anderson, K. C.;

https://doi.org/10.1021/acs.jmedchem.1c00046
J. Med. Chem. 2021, 64, 5886−5904

Carrasco, D. R. BCL9 promotes tumor progression by conferring enhanced proliferative, metastatic, and angiogenic properties to cancer cells. *Cancer Res.* **2009**, *69*, 7577−7586.
(37) Deka, J.; Wiedemann, N.; Anderle, P.; Murphy-Seiler, F.; Bultinck, J.; Eyckerman, S.; Stehle, J.-C.; André, S.; Vilain, N.; Zilian, O.; Robine, S.; Delorenzi, M.; Basler, K.; Aguet, M. Bcl9/Bcl9l are critical for Wnt-mediated regulation of stem cell traits in colon epithelium and adenocarcinomas. *Cancer Res.* **2010**, *70*, 6619−6628.
(38) Brembeck, F. H.; Wiese, M.; Zatula, N.; Grigoryan, T.; Dai, Y.; Fritzmann, J.; Birchmeier, W. BCL9-2 promotes early stages of intestinal tumor progression. *Gastroenterology* **2011**, *141*, 1359−1370.
(39) Moor, A. E.; Anderle, P.; Cantù, C.; Rodriguez, P.; Wiedemann, N.; Baruthio, F.; Deka, J.; André, S.; Valenta, T.; Moor, M. B.; Győrffy, B.; Barras, D.; Delorenzi, M.; Basler, K.; Aguet, M. BCL9/9L-β-catenin signaling is associated with poor outcome in colorectal cancer. *EBioMedicine* **2015**, *2*, 1932−1943.
(40) Gay, D. M.; Ridgway, R. A.; Müller, M.; Hodder, M. C.; Hedley, A.; Clark, W.; Leach, J. D.; Jackstadt, R.; Nixon, C.; Huels, D. J.; Campbell, A. D.; Bird, T. G.; Sansom, O. J. Loss of BCL9/9l suppresses Wnt driven tumourigenesis in models that recapitulate human cancer. *Nat. Commun.* **2019**, *10*, 723.
(41) Mieszczanek, J.; van Tienen, L. M.; Ibrahim, A. E. K.; Winton, D. J.; Bienz, M. Bcl9 and Pygo synergise downstream of Apc to effect intestinal neoplasia in FAP mouse models. *Nat. Commun.* **2019**, *10*, 724.
(42) Kawamoto, S. A.; Coleska, A.; Ran, X.; Yi, H.; Yang, C.-Y.; Wang, S. Design of triazole-stapled BCL9 α-helical peptides to target the β-catenin/B-cell CLL/lymphoma 9 (BCL9) protein-protein interaction. *J. Med. Chem.* **2012**, *55*, 1137−1146.
(43) Takada, K.; Zhu, D.; Bird, G. H.; Sukhdeo, K.; Zhao, J.-J.; Mani, M.; Lemieux, M.; Carrasco, D. E.; Ryan, J.; Horst, D.; Fulciniti, M.; Munshi, N. C.; Xu, W.; Kung, A. L.; Shivdasani, R. A.; Walensky, L. D.; Carrasco, D. R. β-catenin complex inhibits oncogenic Wnt signaling. *Sci. Transl. Med.* **2012**, *4*, 148ra117.
(44) Feng, M.; Jin, J. Q.; Xia, L.; Xiao, T.; Mei, S.; Wang, X.; Huang, X.; Chen, J.; Liu, M.; Chen, C.; Rafi, S.; Zhu, A. X.; Feng, Y. X.; Zhu, D. Pharmacological inhibition of β-catenin/BCL9 interaction overcomes resistance to immune checkpoint blockades by modulating T(reg) cells. *Sci. Adv.* **2019**, *5*, No. eaau5240.
(45) Sang, P.; Zhang, M.; Shi, Y.; Li, C.; Abdulkadir, S.; Li, Q.; Ji, H.; Cai, J. Inhibition of β-catenin/B cell lymphoma 9 protein-protein interaction using α-helix-mimicking sulfono-γ-AApeptide inhibitors. *Proc. Natl. Acad. Sci. U.S.A.* **2019**, *116*, 10757−10762.
(46) de la Roche, M.; Rutherford, T. J.; Gupta, D.; Veprintsev, D. B.; Saxty, B.; Freund, S. M.; Bienz, M. An intrinsically labile α-helix abutting the BCL9-binding site of β-catenin is required for its inhibition by carnosic acid. *Nat. Commun.* **2012**, *3*, 680.
(47) Hoggard, L. R.; Zhang, Y.; Zhang, M.; Panic, V.; Wisniewski, J. A.; Ji, H. Rational design of selective small-molecule inhibitors for β-catenin/B-cell lymphoma 9 protein-protein interactions. *J. Am. Chem. Soc.* **2015**, *137*, 12249−12260.
(48) Zhang, M.; Wang, Z.; Zhang, Y.; Guo, W.; Ji, H. Structure-based optimization of small-molecule inhibitors for the β-catenin/B-cell lymphoma 9 protein-protein Interaction. *J. Med. Chem.* **2018**, *61*, 2989−3007.
(49) Wisniewski, J. A.; Yin, J.; Teuscher, K. B.; Zhang, M.; Ji, H. Structure-based design of 1,4-dibenzoylpiperazines as β-catenin/B-cell lymphoma 9 protein-protein interaction inhibitors. *ACS Med. Chem. Lett.* **2016**, *7*, 508−513.
(50) Zhang, M.; Wisniewski, J. A.; Ji, H. AlphaScreen selectivity assay for β-catenin/B-cell lymphoma 9 inhibitors. *Anal. Biochem.* **2015**, *469*, 43−53.
(51) Vacondio, F.; Silva, C.; Mor, M.; Testa, B. Qualitative structure-metabolism relationships in the hydrolysis of carbamates. *Drug Metab. Rev.* **2010**, *42*, 551−589.
(52) Bagley, S. W.; Brandt, T. A.; Dugger, R. W.; Hada, W. A.; Hayward, C. M.; Liu, Z. Phenyl substituted piperidine compounds for use as ppar activators. WO 2004048334 A1, 2004.
(53) Ammazzalorso, A.; De Filippis, B.; Giampietro, L.; Amoroso, R. N-acylsulfonamides: Synthetic routes and biological potential in medicinal chemistry. *Chem. Biol. Drug Des.* **2017**, *90*, 1094−1105.
(54) Kaelin, W. G., Jr. Common pitfalls in preclinical cancer target validation. *Nat. Rev. Cancer* **2017**, *17*, 441.
(55) Lyou, Y.; Habowski, A. N.; Chen, G. T.; Waterman, M. L. Inhibition of nuclear Wnt signalling: challenges of an elusive target for cancer therapy. *Br. J. Pharmacol.* **2017**, *174*, 4589−4599.
(56) Wang, Z.; Li, Z.; Ji, H. Direct targeting of β-catenin in the Wnt signaling pathway: current progress and perspectives. *Med. Res. Rev.* **2021**, DOI: 10.1002/med.21787.
(57) Sampietro, J.; Dahlberg, C. L.; Cho, U. S.; Hinds, T. R.; Kimelman, D.; Xu, W. Crystal structure of a β-catenin/BCL9/Tcf4 complex. *Mol. Cell* **2006**, *24*, 293−300.
(58) Souers, A. J.; Leverson, J. D.; Boghaert, E. R.; Ackler, S. L.; Catron, N. D.; Chen, J.; Dayton, B. D.; Ding, H.; Enschede, S. H.; Fairbrother, W. J.; Huang, D. C. S.; Hymowitz, S. G.; Jin, S.; Khaw, S. L.; Kovar, P. J.; Lam, L. T.; Lee, J.; Maecker, H. L.; Marsh, K. C.; Mason, K. D.; Mitten, M. J.; Nimmer, P. M.; Oleksijew, A.; Park, C. H.; Park, C.-M.; Phillips, D. C.; Roberts, A. W.; Sampath, D.; Seymour, J. F.; Smith, M. L.; Sullivan, G. M.; Tahir, S. K.; Tse, C.; Wendt, M. D.; Xiao, Y.; Xue, J. C.; Zhang, H.; Humerickhouse, R. A.; Rosenberg, S. H.; Elmore, S. W. ABT-199, a potent and selective BCL-2 inhibitor, achieves antitumor activity while sparing platelets. *Nat. Med.* **2013**, *19*, 202−208.
(59) Mihalyova, J.; Jelinek, T.; Growkova, K.; Hrdinka, M.; Simicek, M.; Hajek, R. Venetoclax: A new wave in hematooncology. *Exp. Hematol.* **2018**, *61*, 10−25.
(60) Nikolovska-Coleska, Z.; Wang, R.; Fang, X.; Pan, H.; Tomita, Y.; Li, P.; Roller, P. P.; Krajewski, K.; Saito, N. G.; Stuckey, J. A.; Wang, S. Development and optimization of a binding assay for the XIAP BIR3 domain using fluorescence polarization. *Anal. Biochem.* **2004**, *332*, 261−273.

https://doi.org/10.1021/acs.jmedchem.1c00046
J. Med. Chem. 2021, 64, 5886−5904